

# PYRREGULAR: A Unified Framework for Irregular Time Series, with Classification Benchmarks

Francesco Spinnato  
University of Pisa, Pisa, Italy

Cristiano Landi  
University of Pisa, Pisa, Italy

## Abstract

Irregular temporal data, characterized by varying recording frequencies, differing observation durations, and missing values, presents significant challenges across fields like mobility, healthcare, and environmental science. Existing research communities often overlook or address these challenges in isolation, leading to fragmented tools and methods. To bridge this gap, we introduce a unified framework, and the first standardized dataset repository for irregular time series classification, built on a common array format to enhance interoperability. This repository comprises 34 datasets on which we benchmark 12 classifier models from diverse domains and communities. This work aims to centralize research efforts and enable a more robust evaluation of irregular temporal data analysis methods.

## 1 Introduction

High-dimensional temporal data is increasingly accessible to decision-makers, domain experts, and researchers [70]. It is vital in fields like mobility, healthcare, and environmental science to capture dynamic changes over time. Yet, variations in recording frequencies, durations across sensors, and occasional failures lead to signals with unequal lengths, gaps, and missing values [32]. These traits make real-world temporal data irregular and difficult to manage [44].

Several research communities address the challenge of irregular temporal data from different perspectives, as its analysis depends heavily on the task, application setting, and modeling approach. As a result, the problem spans multiple fields, including mobility analytics [16], irregular time series classification [42], forecasting [79], and imputation [53, 48], to name a few. Due to this vast amount of tasks, and despite some shared challenges, communities working on irregular temporal data tend to be separated, whereas easier interaction could foster new ideas and accelerate advancements in the field. Each community relies on its own set of techniques, such as traditional statistical or data mining models, neural networks [78], or differential equations [63], often resulting in domain-specific tools and libraries. This is not inherently a drawback, but can lead to fragmented research efforts. The challenges of irregular temporal data are amplified in supervised learning, where standardized benchmarks are notably lacking. While repositories exist for *regular* time series classification [17, 5], regression [73], and forecasting [26], truly *irregular* datasets, capturing real-world missingness and variability, remain scarce. Researchers often resort to artificially manipulated datasets [79], introducing assumptions that overlook structural missingness tied to data collection. As a result, experimental findings have limited applicability [57], and many studies rely on a narrow range of datasets, reducing the generalizability of their methods.

We bridge the gap between research communities by introducing `pyrregular`<sup>1</sup>, a unified framework that offers a comprehensive view of irregular time series. **(I)** We introduce a taxonomy for different kinds of irregularities and propose a dataset structure based on a common array format to enhance interoperability across diverse tools and libraries. This structure is well-suited for handling, visualizing,

<sup>1</sup>The code is available at: <https://github.com/fspinna/pyrregular>.

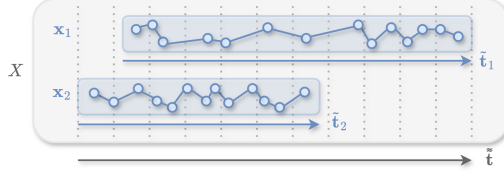


Figure 1: An example of an irregular time series,  $X$ , comprising two signals  $x_1, x_2$  with indices  $\tilde{t}_1, \tilde{t}_2$ , and the combined shared index  $\tilde{t}$ .

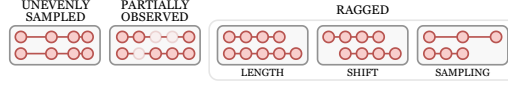


Figure 2: Different kinds of irregularity shown on a multivariate time series with 2 signals and containing up to 5 timestamps. Missing values are depicted as faded red if they were expected to be recorded, while they are omitted if they are caused by raggedness.

and modeling irregular time series data and makes it possible to use it with the vast array of tools already available for time series analysis. (2) We introduce the first standardized dataset repository for irregular time series classification, and (3) we leverage this repository to propose the first generalized benchmark for leading state-of-the-art classifiers alongside several baseline models from different research domains, in an effort to centralize research on this topic. Specifically, we curate 34 irregular time series datasets and evaluate 12 time series classifiers. Our goal is to empower users to seamlessly explore and evaluate a wide range of libraries to address the challenges of irregular temporal data.

## 2 Organizing Irregularity

To develop a unified framework for irregular time series, we must first clarify which types of irregularities we intend to address. As our first contribution, we propose a systematic taxonomy that clearly distinguishes among different forms of irregularity. We begin by defining a time series signal.

**Definition 2.1** (Time Series Signal). A signal (or channel) is a sequence of  $\tau$  observations, each associated to a timestamp, i.e.,  $\mathbf{x} = [(x_1, t_1), \dots, (x_\tau, t_\tau)] = [x_{t_1}, \dots, x_{t_\tau}] \in \mathbb{R}^\tau$ .

A single signal can be *irregular* for two reasons: *uneven sampling*, when at least one interval  $t_{k+1} - t_k$  differs from a constant  $\Delta t$ , and *partially observed*, when expected values are missing and marked as  $NaN$ . The set of real numbers extended with the  $NaN$  symbol is here represented as  $\mathbb{R}$ . We denote with  $\tilde{\mathbf{t}} = [t_1, \dots, t_\tau] \in \mathbb{R}^\tau$ , the sorted collection of all timestamps where an observation of signal  $\mathbf{x}$  was, or should have been recorded, and with  $\tau = |\tilde{\mathbf{t}}|$  the number of observations.

**Definition 2.2** (Time Series). A time series is a collection of  $d$  signals,  $X = \{\mathbf{x}_1, \dots, \mathbf{x}_d\} \in \mathbb{R}^{d \times T}$ .

Time series timestamps are the sorted union of all signal timestamps, i.e.,  $\tilde{\mathbf{t}} = \bigcup_{j=1}^d \tilde{\mathbf{t}}_j \in \mathbb{R}^T$ , with  $T = |\tilde{\mathbf{t}}|$ , as shown in Figure 1. In addition to these intrinsic irregularities, tensor representations introduce a third, structural type: *raggedness*, that is the necessity of padding due to length, sampling, or alignment mismatches between signals. Hence, there are three independent irregularity causes: *uneven sampling*, *partial observation*, and *raggedness*, as depicted in Figure 2. While these categories have appeared informally in prior literature, here we systematically show that they are independent: none implies the others. Unevenly sampled time series do not necessarily imply the presence of partially observed data, as seen in Figure 2 (left). This commonly happens in trajectory data, where the timestamps are usually highly uneven, but shared across the latitude and longitude signals. Vice versa, the presence of unobserved data does not imply uneven timestamps, as an observation may be accidentally missing from an overall constant sampling. Finally, neither unevenly sampled nor partially observed data imply raggedness. In the example shown in Figure 2, the two leftmost time series could be stored in  $2 \times 4$  and  $2 \times 5$  matrices, respectively, without requiring any padding.

Raggedness is a kind of irregularity that can naturally arise even when dealing with completely observed data sampled at equal time intervals, because of different issues created when storing a multivariate time series in an array-like structure. As so, a single, univariate signal cannot be ragged by itself. In general, raggedness arises when at least two signals,  $a$  and  $b$ , do not share the same timestamps, i.e.,  $\tilde{\mathbf{t}}_a \neq \tilde{\mathbf{t}}_b$ . We identify three independent fundamental reasons for why this can happen. The first is *ragged length*, when  $a$  and  $b$  have a different number of observations:  $|\tilde{\mathbf{t}}_a| \neq |\tilde{\mathbf{t}}_b|$ . The second is *shift*, where at least one signal starts and ends before another:  $(t_{a,1} < t_{b,1}) \wedge (t_{a,\tau_a} < t_{b,\tau_b})$ . The third is *ragged sampling*, when at least one element of the sampling intervals differs between two signals, i.e.,  $\Delta t_{a,k} \neq \Delta t_{b,k}$  for some  $k$ , where  $\Delta t_{a,k} = t_{a,k+1} - t_{a,k}$  and  $\Delta t_{b,k} = t_{b,k+1} - t_{b,k}$ .

Again, none of these, by itself, implies the other, as depicted in Figure 2. Combinations of these issues yield highly irregular data, where *NaN* can indicate either a missing value in a partially observed time series or padding due to raggedness in tensor storage. Moreover, raggedness can exist also in a time series dataset, i.e., a collection of  $n$  time series,  $\mathcal{X} = \{X_1, \dots, X_n\} \in \mathbb{R}^{n \times d \times \mathcal{T}}$ , as all instances share the same sorted timestamps,  $\mathbf{t} = \bigcup_{i=1}^n \tilde{\mathbf{t}}_i \in \mathbb{R}^{\mathcal{T}}$ , with  $\mathcal{T} = |\mathbf{t}|$ . The *timestamp index* for the whole dataset is denoted as  $\mathbf{k} = [1, \dots, \mathcal{T}]$ .

Associated with time series datasets are often *static attributes*, which refer to information linked to individual instances that remain independent of the time dimension. For example, in a medical dataset, static variables might include the patient’s demographic details. These attributes can also serve as targets in supervised tasks. This work focuses on classification tasks, i.e., targets are categorical.

### 3 Related Work

**Datasets and Benchmarks.** There is a significant divide in the literature in the availability of datasets and benchmarking efforts, between *regular* and *irregular* time series data. Supervised learning for *regular* time series data is extensively addressed in the literature. From a survey perspective, numerous “bake-offs” [7, 65, 56] have benchmarked state-of-the-art classifiers on hundreds of standard datasets from the famous UEA and UCR repositories [17, 5]. On the contrary, the benchmarking literature on *irregular* time series remains limited. While secondary sources, such as [79, 78], offer surveys on specific tasks like irregular time series imputation, comprehensive benchmarks for downstream tasks like classification are largely confined to primary studies [42, 69, 22, 13]. Even within these studies, evaluations are often performed on a small number of datasets. Moreover, benchmark datasets are not always inherently irregular; instead, they are commonly derived from regular datasets through simulation, i.e., dropping valid observations [79]. Although this strategy can, when executed correctly, create irregular time series, introducing missingness is a non-trivial process requiring careful decisions about the type of missingness to simulate [64]. Adding to these challenges, a recent study [57] highlighted that most research neglects structural missingness, referring to non-random, multivariate patterns of missingness within datasets. Such patterns can only be faithfully retained by preserving the original data with minimal alterations.

**Libraries.** Regarding *regular* time series data, Python libraries such as `sktime` [51], `aeon` [55], and `tslearn` [74] provide a wide range of classifier implementations, along with access to the UEA and UCR repositories, enabling systematic and reproducible evaluations. Although some of these datasets contain irregularities, the typical approach involves imputing missing values and discarding timestamps during downstream tasks. The most prominent Python library for *irregular* time series analysis is `pypots` [21]. `pypots` offers several classifiers, a few partially observed time series datasets, and provides an interface for adding missingness in regular datasets. A limitation of `pypots` is that it overlooks irregularity from uneven sampling, ignoring timestamps. It also operates within its own ecosystem, lacking interfaces for cross-library comparisons. This makes benchmarking against `sktime` models or using irregular datasets with libraries like `aeon` difficult, due to incompatible data formats and requirements, hindering standardization efforts. The primary reason for these challenges is the difficulty in managing irregular time series due to high dimensionality, missing values, and timestamps. Most libraries for time series prediction require dense 3D tensors to represent time series, signals, and identifiers (IDs), often demanding extensive padding and increased memory usage. To mitigate this, many libraries implement special arrays to represent missing values or variable-length instances. For example, `numpy` masked arrays [30] indicate valid entries with masks but are memory-inefficient since they store both data and masks. Alternatives include `awkward` arrays [60], `jagged` `pytorch` arrays [59], `ragged` `tensorflow` arrays [1], `zarr`, `pyarrow`, or `sparse` arrays [2]. Although efficient in managing varied-sized data, these structures cannot inherently handle timestamps. Forecasting libraries like `nixtla` or `gluonTS` [3] typically use a *long format*, representing data as tuples  $(i, j, t, x)$  with instance and signal IDs, timestamps, and observed values. While efficient for forecasting, this format requires pivoting for classification tasks, and static variables are either duplicated or stored separately, causing inefficiencies. Lastly, `xarray` [33] supports timestamped multi-dimensional arrays but lacks native support for sparse, irregular data.

In summary, to the best of our knowledge, no existing array format is able to represent irregular time series data in all its nuances, hindering interaction between different time series communities. Given these limitations, we introduce a framework that acts as a compatibility layer built on a unified array format, enabling seamless interoperability between existing time series libraries.

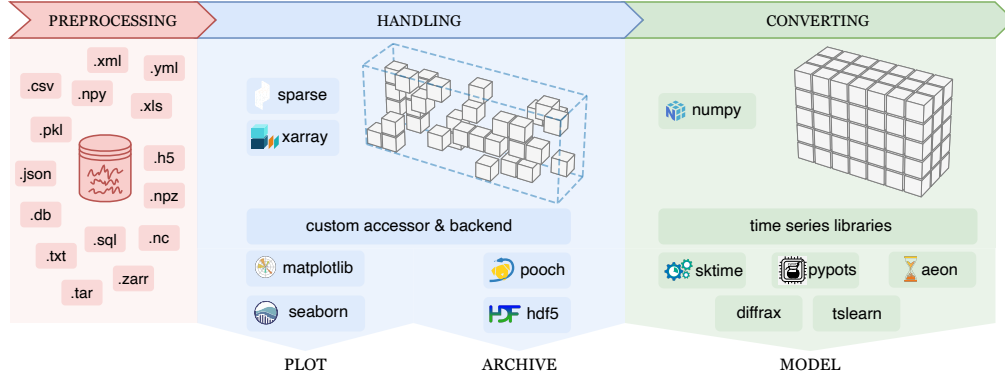


Figure 3: A simplified schema of our framework. (left) Data from different sources is preprocessed and represented in our proposed array container (center), which combines `xarray` with an underlying `sparse` tensor via a custom accessor and backend. This container can be easily manipulated, plotted, and stored. (right) Finally, it can also be converted into a more common dense representation, which can be used for downstream tasks with any standard time series library.

## 4 A Unified Framework for Irregular Time Series

This work addresses the gap in the literature on irregular time series by introducing an efficient container specifically designed for such data. This facilitates the integration of methods and datasets from various research communities into a unified framework. We outline key aspects of this solution. (i) *Ease of Use*: the framework supports several stages of the data science workflow, including visualization, preprocessing with classical and temporal slicing, and seamless conversion to dense arrays used in leading machine learning libraries. (ii) *Robustness*: the implementation leverages established and well-maintained libraries, as there is no point in reinventing the wheel. (iii) *Flexibility*: the container supports all kinds of time series irregularities. (iv) *Replicability*: to ensure comparable results, preprocessing is standardized, addressing the variability in irregular datasets. A depiction of the three steps of `pyrregular` is shown in Figure 3: *preprocessing*, where the original irregular data is transformed into our proposed container; *handling*, where the data can be explored, manipulated, and stored; and *converting*, where the data is prepared for downstream tasks.

**Preprocessing.** The first step in our framework involves preprocessing and transforming irregular time series datasets into the proposed representation. Irregular time series data can be found in a wide variety of sources and formats (Figure 3, left), presenting unique challenges in terms of parsing, handling, and extracting the relevant temporal and feature information. Regardless of the original data structure, our framework requires only a function capable of yielding the data in the standardized long format. In this representation, each row captures the time series ID, signal ID, timestamp, and observed value:  $(i, j, t, x)$ . The core intuition behind our approach is that the long format closely resembles the sparse coordinate (COO) representation [23].

The COO format, as implemented by `sparse` [2], can efficiently encode sparse 3D tensors, by using indices for the time series, signal, and timestamp, accompanied by an observed value entry, formally  $(i, j, k, x)$ . The key distinction between the long format and the COO representation lies in the handling of the timestamps: while the COO format requires discrete timestamp indices,  $k$ , the long format uses real-valued timestamps,  $t$ . An example is reported in Figure 4 (left). This difference, however, can be easily bridged by mapping the timestamps,  $t$ , to discrete positions within the COO array,  $k$ . Formally, given the timestamps vector  $\mathbf{t} = [t_1, \dots, t_T]$ , each timestamp can be mapped to its corresponding position (index), in the COO format as  $\mathbf{k} = [1, \dots, T]$  (and vice-versa), as depicted in Figure 4 (center). With this mapping, converting between the long format and the COO representation can be easily accomplished, as the time series dataset is read once to construct the mapping and a second time to incrementally build the COO matrix by yielding each row as it is generated (Figure 4, right). Practitioners need only to define a custom function that, given their own data, incrementally produces rows in the long format. Even when the initial dataset is not organized in this manner, the conversion to the long format is typically straightforward. This process ensures uniformity across input formats and transparency, as the preprocessing steps are explicitly documented in this

function, and can be reproduced at any time. Though it may be runtime-intensive, this step needs to be performed only once, after which the library streamlines all subsequent transformations and processing. The output after preprocessing is a sparse tensor, denoted as  $\mathcal{X} \in \mathbb{R}^{n \times d \times T}$ .

**Handling.** The COO representation offers advantages over the classical long format. First, it supports array-like operations with reasonable performance, including reshaping and slicing. Moreover, it allows for rapid conversion to task-specific array structures, such as other sparse formats like GCXS [68]. Compared to classical dense arrays, its primary advantage lies in memory efficiency, as only the recorded observations are stored. All padding is represented by a *fill value* and remains implicit, meaning it is not directly stored but is generated only when the sparse array is transformed into a dense form. Commonly, the fill value is set to zero. However, we propose setting it to *NaN* to model *raggedness*. Further, the COO format naturally accommodates partially observed data by explicitly storing a fill value. This allows for distinguishing between the two types of missing data previously discussed. Specifically, an explicitly stored fill value, i.e., a row  $(i, j, k, \text{NaN})$ , can indicate a missing entry that should be present, while implicit *NaNs* reflect missingness due to data raggedness. In this sense, the COO tensor by itself is enough to represent both ragged and partially observed time series.

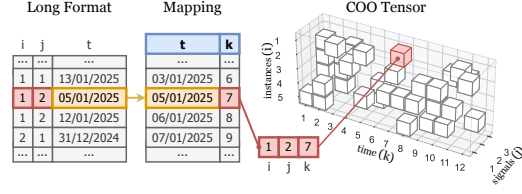


Figure 4: Long format to COO tensor conversion process. Each row of the long format is processed to retrieve the absolute position  $k$  of a given timestamp  $t$ . The triplet, instance ID ( $i = 1$ ), signal ID ( $j = 2$ ), and timestamp index ( $k = 7$ ), is used to populate the sparse COO tensor.

However, to capture an unevenly sampled time series, it is also essential to store the timestamps. To achieve this, we can leverage our timestamp to COO ( $t$  to  $k$ ) mapping using `xarray` (Figure 3, center). In particular, we use `xarray` [33] to store the timestamps and extend it to utilize an underlying sparse COO tensor internally. These functionalities are possible through our custom backend and accessor, which extend the `xarray` library, to support sparse arrays. Further, `xarray` naturally facilitates the storage of static attributes linked to any dataset dimension, such as class labels in classification tasks. In this way, the entire time series dataset, comprehensive of the timestamps and any static attribute, is represented as a single object. Overall, this approach offers significant storage efficiency, particularly given the typically high data sparsity, and ensures ease of use by supporting all existing `xarray` functions like timestamp range queries. Further, the accessor enables plotting, while the backend allows direct saving and loading to a hierarchical data format, locally or online, via `pooch` [76], eliminating the need to perform the preprocessing step again.

**Converting.** Despite its advantages, `xarray` is not directly supported by most libraries for supervised learning tasks. Therefore, it is crucial to demonstrate how this array structure can be efficiently prepared for such applications. Specifically, for classification tasks,  $\mathcal{X} \in \mathbb{R}^{n \times d \times T}$  should be transformed into a dense tensor that minimizes raggedness while preserving the inherent missingness from partially observed time series and maintaining the order of observations within the same time series. This conversion is important because, in classification tasks, raggedness is typically irrelevant to the target and would otherwise result in excessively large dense arrays filled predominantly with *NaNs*. For instance, particularly in classification tasks, the specific starting dates of time series, such as  $a$  beginning on January 23rd and  $b$  on January 30th, are typically irrelevant. In such a case, we aim to avoid introducing 7 *NaN* values at the beginning of time series  $b$ . For a COO array, this transformation corresponds to a dense ranking operation on the timestamp index,  $k$ , performed time series-wise. Formally, for each COO entry  $(i, j, k, x)$ , we produce  $(i, j, \text{rank}_i(k), x)$ , where:

$$\text{rank}_i(k) = 1 + |\{k' \in [1, T_i] : k' < k\}|.$$

This process shifts the timestamp indices within each time series,  $X_i$ , into a consecutive sequence ranging from 1 to its length,  $T_i$ . As a result, the tensor  $\mathcal{X} \in \mathbb{R}^{n \times d \times T}$  can be densified into a more compact,  $\mathcal{X}' \in \mathbb{R}^{n \times d \times T}$ , where  $T = \max_i(T_i)$ . This ensures minimal padding, with the timestamp dimension set to the maximum number of timestamps in any time series. Further, for models that support it, the timestamps can be concatenated as an additional channel [42].  $\mathcal{X}'$  can be used by any downstream library, in our case, time series classification libraries. Specifically, we currently support `sktime` [51], `aeon` [55], `tslearn` [74], `pytots` [21] and `diffraX` [41].

Table 1: Datasets used for our benchmarks, divided by irregularity type: unevenly sampled (US), partially observed (PO), unequal length (UL), shift (SH), ragged sampling (RS).

	health			human activity recognition										mobility						sensor			other			synth									
	MI3	P12	P19	CT	GM1	GM2	GM3	GP1	GP2	GX	GY	GZ	LPA	PAM	PGZ	SGZ	AN	AOC	APT	ARC	GS	MP	SE	TA	VE	DD	DG	DW	IW	JV	PGE	PL	SAD	ABF	
US	✓	✓	✓	✗	✗	✗	✗	✗	✗	✗	✗	✗	✓	✓	✗	✗	✓	✗	✗	✗	✓	✗	✓	✓	✓	✗	✗	✗	✗	✗	✓	✗	✗	✗	✓
PO	✓	✓	✓	✗	✗	✗	✗	✗	✗	✗	✗	✗	✗	✓	✗	✗	✗	✗	✗	✗	✗	✗	✗	✗	✗	✓	✓	✓	✗	✗	✗	✗	✗	✗	✗
UL	✓	✓	✓	✓	✓	✓	✓	✓	✓	✓	✓	✓	✓	✓	✓	✓	✓	✓	✓	✓	✓	✓	✓	✓	✓	✗	✗	✗	✓	✓	✓	✓	✓	✓	✗
SH	✓	✓	✓	✗	✗	✗	✗	✗	✗	✗	✗	✗	✓	✓	✗	✗	✗	✗	✗	✗	✓	✗	✓	✓	✗	✗	✗	✗	✗	✗	✓	✗	✗	✗	✗
RS	✓	✓	✓	✗	✗	✗	✗	✗	✗	✗	✗	✗	✓	✓	✗	✗	✓	✗	✗	✗	✓	✗	✓	✓	✓	✗	✗	✗	✗	✗	✓	✗	✗	✗	✗

Table 2: Summary of evaluated classifiers.

Library		Model	Type	Domain
aeon	[72]	BORF	dictionary-based transform + LGBM classifier	regular, ragged
		RIFC	interval-based transform + LGBM classifier	partially observed
diffraX	[42]	NCDE	neural controlled differential equations	unevenly sampled
pypots	[9]	BRITS	bidirectional recurrent imputation network	partially observed
	[11]	GRU-D	gated recurrent unit with decay	partially observed
	[83]	RAINDROP	graph neural network	partially observed
	[22]	SAITS	self-attention-based imputation transformer	partially observed
	[81]	TIMESNET	temporal 2d-variation transformer.	partially observed
sktime	[40]	LGBM	gradient boosted tree	tabular
	[20]	ROCKET	kernel-based transform + LGBM classifier	regular
	[4]	SVM	support vector machine with distance kernel	regular, ragged
tslearn	[67]	KNN	distance-based with dynamic time warping	regular, ragged

## 5 Classification Benchmarks

We present a comprehensive benchmark enabled by `pyrregular`, in which we evaluate 12 classifiers from a variety of time series libraries on a curated collection of 34 irregular time series datasets. We assess model performance from multiple perspectives, including dataset characteristics, robustness across irregularity types, and the potential for performance improvement through fine-tuning.

**Datasets.** We select diverse, naturally irregular datasets, without removing or altering any observation to induce irregularity (Table 1). First, our collection contains widely used irregular time series classification datasets: *PhysioNet 2012* (P12) [71], *PhysioNet 2019* (P19) [62], and the *MIMIC-III* (MI3) clinical database [39] from the medical domain, as well as *Pamap2* (PAM) [61] for physical activity monitoring. Additionally, we include the 11 variable-length univariate time series classification problems [28, 10, 54, 25] from [6], the 4 partially observed datasets [34, 15] from [56], and the 7 variable-length multivariate time series classification problems [18, 80, 12, 45, 29] from [65]. We also provide datasets that, to the best of our knowledge, were never used in these kinds of benchmarks. These include data for trajectory classification of entities such as mammals (AN)[24], birds (SE) [8], and vehicles like buses and trucks (VE), taxis [58] (TA) and combinations of the previous [86] (GS). Further, we include a small dataset about the productivity prediction for garment employees [35] (PGE), and a human activity recognition dataset [77] (LPA). Finally, inspired by the classical Cylinder-Bell-Funnel benchmark [66] for regular time series classification, we introduce an irregular version called *Alembics-Bowls-Flasks* (ABF), in which the class depends on the skewness of the time sampling. Where available, we use the default train/test split for training and inference, else we set them based on each dataset description and original paper. More details are provided in Appendix B.

**Models.** The objective of these experiments is to benchmark methods capable of naturally handling irregular time series without introducing bias through imputation techniques. For this reason, and to keep the benchmarks to a reasonable amount, we limit our evaluation to classifiers that inherently support irregular inputs and are available in the aforementioned libraries (Table 2). As classical baselines, we use K-Nearest Neighbors (KNN) with Dynamic Time Warping [67], a time series



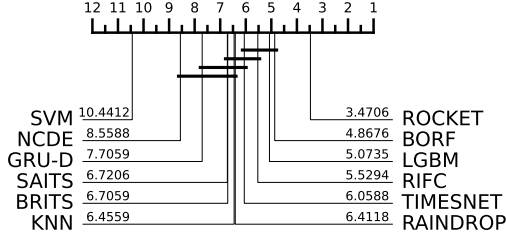


Figure 5: CD plot for the benchmarked models in terms of F1. Best models to the right. Connected models are statistically tied.

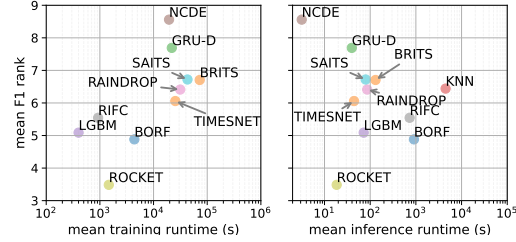


Figure 6: Mean F1 rank against training and inference runtimes for the top 11 models across all datasets. The best models are on the bottom left.

Support Vector Machine (SVM) with a Longest Common Subsequence (LCSS) kernel [4], and a LightGBM classifier (LGBM) trained directly on raw time series, ignoring temporal dependencies. For regular time series models, we include the Bag-Of-Receptive-Fields (BORF) [72] from *aeon*, ROCKET [19, 20] via its MINIROCKET version in *sktime*, and a Random Interval Feature Classifier (RIFC). These models transform the data and rely on downstream classifiers; we use LGBM to handle possible *NaN*s. For partially observed data, we benchmark GRU-D [11], BRITS [9], RAINDROP [83], two transformer models, SAITS [22] and TIMESNET [82], from *pypots*, and a Neural Controlled Differential Equation model (NCDE) [42] from *diffra*. More details are provided in Appendix B.

**Experimental Setup.** Following standard practice in similar benchmarking studies [7, 65, 56], all models are trained using the default hyperparameters provided by their respective libraries or those recommended in the original papers. The goal of this benchmark, consistent with prior bake-offs, is to identify the model that best generalizes with a single, reasonable parameter configuration rather than fine-tuning each model for individual datasets. For this reason, the results of these benchmarks do not necessarily highlight the best possible model for a given task, but the model that generalizes best in many. Each model is allocated two weeks ( $\approx 20000$  minutes) for training and inference on each dataset, with access to 32 cores and 512 GB of memory, and to a GPU when the model can use it<sup>2</sup>. Experiments are repeated three times for highly stochastic models, and the average performance is maintained. Although accuracy is the most commonly used metric for evaluating classification performance, we have chosen the F1 score with macro averaging as our primary performance metric. The F1 score is more robust in the presence of unbalanced datasets [37], such as some of the ones provided. Accuracy results, along with additional metrics, statistical tests, and plots, are reported in Appendix C and are consistent with the findings presented below.

## 5.1 Results and Discussion.

We present a comparative analysis of the aggregate results of the benchmark outcomes. We report a critical difference (CD) plot in Figure 5, which ranks models in terms of F1. Models are arranged from right to left, with lower ranks indicating better performance. Models connected by a horizontal bar are statistically tied under a one-sided Holm-corrected Wilcoxon signed-rank test with a significance threshold of 0.05. ROCKET emerged as the clear top-performing model, demonstrating consistent superiority across the datasets. Even if this result aligns with its established reputation as one of the best models for *regular* time series classification [56], its efficacy on *irregular* data is somewhat surprising, as ROCKET does not exploit any information about said irregularity. Following ROCKET, a cluster of methods, including BORF, LGBM, RIFC, TIMESNET, exhibits statistically tied performance. Lower ranks are occupied by RAINDROP, KNN, BRITS, followed by GRU-D and NCDE, with SVM distinctly identified as the worst-performing model.

**Performance vs. Time.** Besides predictive performance, runtime is also a significant factor. In Figure 6, we compare the average F1 rank against training and inference runtimes, discarding SVM for better readability. The better-performing, faster models appear in the bottom-left region of the plot. In terms of training, LGBM is the fastest, followed by RIFC and ROCKET, with ROCKET also being also very fast during inference. For this reason, ROCKET emerges as the best tradeoff between F1 and runtime. Interestingly, despite being designed for tabular data, LGBM performs well. This

<sup>2</sup>System: IBM SYSTEM POWER AC922 Compute Nodes with  $2 \times 16$ -core 2.7GHz POWER9 CPUs, 512GB of RAM. NVIDIA Tesla V100 32GB GPU

Size	big	4.9	6.6	7.5	5.9	5.6	8.8	6.3	4.9	3.6	6.8	10.0	7.2
	small	4.9	6.8	7.9	7.0	4.6	8.3	6.5	6.2	3.4	6.6	10.9	4.9
Signals	multi	4.6	7.3	8.5	4.7	5.4	9.1	6.4	6.0	2.9	7.1	9.9	6.2
	uni	5.1	6.2	7.0	8.0	4.8	8.1	6.4	5.2	4.0	6.4	10.9	5.9
Length	long	6.8	4.9	6.2	6.8	5.6	8.7	6.4	6.6	4.9	6.5	9.7	5.0
	short	2.8	8.7	9.4	6.0	4.6	8.4	6.4	4.4	1.9	7.0	11.2	7.2
		BORF	BRITS	GRU-D	KNN	LGBM	NODE	RAINDROP	RIFC	ROCKET	SAITS	SVM	TIMESNET

Figure 7: Mean F1 rank (lower is better) against dataset size in terms of instances (top), number of signals (center), and time series length (bottom).

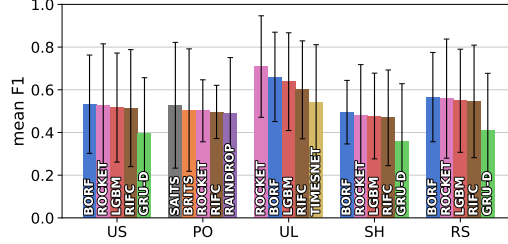


Figure 8: Mean F1 (higher is better) of the 5 best-performing models for each type of irregularity.

finding aligns with observations in [73], where gradient-boosting trees showed strong performance in *regular* time series *regression*. LGBM is a compelling choice due to its decent performance and exceptionally fast training time, making it attractive for practitioners needing quickly fine-tunable baselines. Neural network-based methods, though designed for irregular data, underperform in these bake-off-style benchmarks, except for their competitive inference runtime. Similar patterns appear in regular time series classification [56]. We hypothesize that simpler, *generalist*, models, like ROCKET, excel in bake-off settings due to their low-variance, high-bias inductive bias, making them robust across a wide range of tasks, contrary to *specialized* models, which exhibit strong performance on specific types of irregularity or dataset characteristics, especially after fine-tuning.

**Performance vs. Dimension.** Figure 7 (top) shows the mean F1 ranks of all benchmarked models (lower is better), stratified by dataset size: small (at most 500 instances) and large (more than 500 instances). KNN and RIFC exhibit a noticeable drop in rank on larger datasets, indicating limited scalability or reduced robustness as the number of training examples increases. In contrast, LGBM, and especially TIMESNET, improve significantly in rank, suggesting that more complex models, particularly transformer-based ones, benefit from greater data availability to better exploit their capacity. Figure 7 (center) shows the mean F1 ranks for univariate and multivariate time series. While the best-ranked model is again ROCKET, all neural network-based approaches benefit from increased dimensionality, making them particularly suitable for multivariate time series. Figure 7 (bottom) reports the mean F1 ranks stratified by time series length: short (at most 360 observations) and long (more than 360 observations). Here, recurrent models such as GRU-D and BRITS, along with several other neural architectures, tend to struggle on longer sequences. RAINDROP stands out as an exception, likely owing to its graph-based design. Meanwhile, models that rely on localized or interval-based features, such as ROCKET, RIFC, and especially BORF, show improved performance on longer time series, indicating that in this case, simpler is better.

**Performance vs. Irregularity.** In Figure 8, we report the average F1 score of the top-5 performing models within each irregularity group. ROCKET, BORF, and LGBM consistently rank among the top three across *unevenly sampled*, *unequal length*, *shifted*, and *ragged sampling* time series. GRU-D, while generally ranking lower overall, appears among the top five models in three out of the five groups, showing decent average performance. *Partially observed* time series exhibit markedly different behavior: here, models designed to handle missing data, such as SAITS and BRITS, outperform ROCKET, BORF, and LGBM. This suggests that explicitly modeling missingness can be highly beneficial, particularly for datasets with structured patterns of missing values.

**Performance after Fine-tuning.** In Table 3, we present the average performance of the top three *generalist* models, ROCKET, BORF, and LGBM, evaluated in terms of area under the Receiver Operating Characteristic curve (*auc*) and area under the Precision-Recall curve (*aupr*) following hyperparameter tuning. These evaluations follow the same 5-fold cross-validation setup and are compared against reference results from [83, 49, 50, 84] on the two most commonly used irregular medical datasets (P12) [71] and (P19) [62]. The aim of this benchmark is to assess whether *generalist* classifiers can also be effectively fine-tuned for specific tasks, and to compare them with state-of-the-art *specialist* deep learning models such as CONTIFORMER [13], GRU-D [11], MTSFORMER [84], MUSICNET [50], and RAINDROP [83]. Results indicate that, when optimally fine-tuned, deep learning-based algorithms outperform simpler regular time series classifiers. However, except for ROCKET, which underperforms in this test, this advantage is not always substantial; for instance,



Table 3: Comparison of best-performing models from the bake-off, against baseline reference results (higher is better). Best values in bold, second best underlined.

		BORF	CONTI FORMER	GRU-D	LGBM	MTS FORMER	MUSIC NET	RAIN DROP	ROCKET
P12	<i>auc</i>	74.9±0.0	81.2±0.8	81.9±2.1	78.4±0.0	84.9±1.4	<b>86.1±0.4</b>	82.8±1.7	53.4±0.0
	<i>aupr</i>	33.4±0.0	43.9±3.0	46.1±4.7	38.1±0.0	<u>51.1±3.7</u>	<b>54.1±2.2</b>	44.0±3.0	15.8±0.0
P19	<i>auc</i>	80.1±0.0	79.2±2.3	83.9±1.7	85.2±0.0	<b>88.8±1.5</b>	86.8±1.4	87.0±2.3	77.3±0.0
	<i>aupr</i>	38.1±0.0	35.8±2.3	46.9±2.1	44.1±0.0	<b>57.7±4.4</b>	45.4±2.7	<u>51.8±5.5</u>	35.2±0.0

LGBM achieves the fourth-best score on P19, outperforming models like CONTIFORMER and GRU-D. Another advantage of models such as ROCKET, BORF, and LGBM is that the performance is very stable, with near-zero standard deviation to a single decimal place. This underscores the value of being able to readily apply standard approaches, as they can offer fast, stable, and non-trivial baselines. However, deep learning offers more flexibility for optimizing on specific tasks, with reasonable inference times when aiming for raw performance for deployment purposes.

**Performance vs. Trustworthiness.** Though not the main focus of this work, we briefly address model trustworthiness, crucial in high-stakes fields like healthcare, where irregular data is common. The most interpretable models in our benchmark are BORF, which relies on subsequence presence/absence, and RIFC, which uses simple interval-based features, both explainable via SHAP [52]. Neural models can be interpreted with gradient-based methods, though the reliability of their explanations on irregular data is unexplored. The top-performing model, ROCKET, offers little interpretability and depends on expensive model-agnostic techniques [75]. Robustness to random initialization also matters: models with high variance across seeds hinder reproducibility. Stable methods like LGBM, BORF, and KNN may be preferable in sensitive settings, even at some cost in performance.

## 6 Conclusion

In this work, we presented *pyrregular*, a unified framework for addressing the challenges of irregular time series. By introducing a standardized repository for irregular time series classification and structuring the datasets in a common array format, we provided a cohesive way to work with varying forms of irregularity. Our extensive empirical evaluation of 12 state-of-the-art classifiers and baseline methods on 34 datasets emphasizes both the complexity of this domain and the benefits of a shared benchmarking resource. Results indicate that, with appropriate configuration and tuning, specialist models such as neural networks still attain state-of-the-art performance. However, extending their applicability across diverse tasks remains a significant challenge. Interestingly, simple generalist classifiers originally designed for *regular* time series data, such as ROCKET, perform remarkably well on irregular time series in bake-off-style benchmarks, even without leveraging the irregularity itself. This observation reveals a crucial research gap: the need to develop *generalist* methods capable of explicitly exploiting irregularities, such as timestamp information or the nature of missingness.

The construction of this extensive set of classification benchmarks was significantly facilitated by our unified interface designed to abstract away the complexities of working with irregular time series data across diverse model libraries. By decoupling data handling from model-specific implementations, *pyrregular* mitigates common sources of error and substantially improves the reproducibility of preprocessing pipelines. Despite these benefits, a current limitation of our proposal is its focus on classification tasks, even though irregular time series datasets are equally relevant for regression, forecasting, anomaly detection, imputation, to name a few. Notably, many of the datasets we have curated contain additional target variables that could support such tasks, offering promising opportunities for future exploration. Further, while we aimed to provide a diverse and representative selection of baseline models, our choices were guided by practical considerations, such as library availability and interface compatibility, rather than exhaustive coverage of the literature. We acknowledge that several other relevant baselines could further enrich the comparison. Our goal was not to be fully comprehensive, but to establish a robust and extensible starting point for future benchmarking efforts within a unified framework. Future efforts will extend the framework to support a wider range of tasks, integrate more datasets, and incorporate additional methods from a broader selection of time series libraries, increasing its relevance across diverse research domains.

## References

- [1] Martín Abadi, Ashish Agarwal, Paul Barham, Eugene Brevdo, Zhifeng Chen, Craig Citro, Greg S. Corrado, Andy Davis, Jeffrey Dean, Matthieu Devin, Sanjay Ghemawat, Ian Goodfellow, Andrew Harp, Geoffrey Irving, Michael Isard, Yangqing Jia, Rafal Jozefowicz, Lukasz Kaiser, Manjunath Kudlur, Josh Levenberg, Dandelion Mané, Rajat Monga, Sherry Moore, Derek Murray, Chris Olah, Mike Schuster, Jonathon Shlens, Benoit Steiner, Ilya Sutskever, Kunal Talwar, Paul Tucker, Vincent Vanhoucke, Vijay Vasudevan, Fernanda Viégas, Oriol Vinyals, Pete Warden, Martin Wattenberg, Martin Wicke, Yuan Yu, and Xiaoqiang Zheng. TensorFlow: Large-scale machine learning on heterogeneous systems, 2015.
- [2] Hameer Abbasi. Sparse: A more modern sparse array library. In *SciPy*, pages 65–68, 2018.
- [3] Alexander Alexandrov, Konstantinos Benidis, Michael Bohlke-Schneider, Valentin Flunkert, Jan Gasthaus, Tim Januschowski, Danielle C. Maddix, Syama Rangapuram, David Salinas, Jasper Schulz, Lorenzo Stella, Ali Caner Türkmen, and Yuyang Wang. GluonTS: Probabilistic and Neural Time Series Modeling in Python. *Journal of Machine Learning Research*, 21(116):1–6, 2020.
- [4] Mohammad Ali Bagheri, Qigang Gao, and Sergio Escalera. Support vector machines with time series distance kernels for action classification. In *2016 IEEE Winter Conference on Applications of Computer Vision (WACV)*, pages 1–7. IEEE, 2016.
- [5] Anthony Bagnall, Hoang Anh Dau, Jason Lines, Michael Flynn, James Large, Aaron Bostrom, Paul Southam, and Eamonn Keogh. The uea multivariate time series classification archive, 2018. *arXiv preprint arXiv:1811.00075*, 2018.
- [6] Anthony Bagnall, Michael Flynn, James Large, Jason Lines, and Matthew Middlehurst. On the usage and performance of the hierarchical vote collective of transformation-based ensembles version 1.0 (hive-cote v1. 0). In *Advanced Analytics and Learning on Temporal Data: 5th ECML PKDD Workshop, AALTD 2020, Ghent, Belgium, September 18, 2020, Revised Selected Papers 6*, pages 3–18. Springer, 2020.
- [7] Anthony Bagnall, Jason Lines, Aaron Bostrom, James Large, and Eamonn Keogh. The great time series classification bake off: a review and experimental evaluation of recent algorithmic advances. *Data mining and knowledge discovery*, 31:606–660, 2017.
- [8] Ella Browning, Mark Bolton, Ellie Owen, Akiko Shoji, Tim Guilford, and Robin Freeman. Predicting animal behaviour using deep learning: Gps data alone accurately predict diving in seabirds. *Methods in Ecology and Evolution*, 9(3):681–692, 2018.
- [9] Wei Cao, Dong Wang, Jian Li, Hao Zhou, Lei Li, and Yitan Li. Brits: Bidirectional recurrent imputation for time series. *Advances in neural information processing systems*, 31, 2018.
- [10] Fabio Marco Caputo, Pietro Prebianca, Alessandro Carcangiu, Lucio Davide Spano, and Andrea Giachetti. Comparing 3d trajectories for simple mid-air gesture recognition. *Comput. Graph.*, 73:17–25, 2018.
- [11] Zhengping Che, Sanjay Purushotham, Kyunghyun Cho, David Sontag, and Yan Liu. Recurrent neural networks for multivariate time series with missing values. *Scientific reports*, 8(1):6085, 2018.
- [12] Yanping Chen, Adena Why, Gustavo Batista, Agenor Mafra-Neto, and Eamonn Keogh. Flying insect classification with inexpensive sensors. *Journal of insect behavior*, 27:657–677, 2014.
- [13] Yuqi Chen, Kan Ren, Yansen Wang, Yuchen Fang, Weiwei Sun, and Dongsheng Li. Contiformer: Continuous-time transformer for irregular time series modeling. *Advances in Neural Information Processing Systems*, 36, 2024.
- [14] ChoroChronos Archive. Trucks dataset - dataset and algorithms | choroChronos.org. <http://www.choroChronos.org/>. Accessed: 2025-01-23.
- [15] City of Melbourne. Pedestrian counting system. <http://www.pedestrian.melbourne.vic.gov.au>, 2020. Accessed: 2025-01-23.

- [16] Camila Leite da Silva, Lucas May Petry, and Vania Bogorny. A survey and comparison of trajectory classification methods. In *2019 8th Brazilian conference on intelligent systems (BRACIS)*, pages 788–793. IEEE, 2019.
- [17] Hoang Anh Dau, Anthony Bagnall, Kaveh Kamgar, Chin-Chia Michael Yeh, Yan Zhu, Shaghayegh Gharghabi, Chotirat Ann Ratanamahatana, and Eamonn Keogh. The ucr time series archive. *IEEE/CAA Journal of Automatica Sinica*, 6(6):1293–1305, 2019.
- [18] Vinícius M. A. de Souza. Asphalt pavement classification using smartphone accelerometer and complexity invariant distance. *Eng. Appl. Artif. Intell.*, 74:198–211, 2018.
- [19] Angus Dempster, François Petitjean, and Geoffrey I Webb. Rocket: exceptionally fast and accurate time series classification using random convolutional kernels. *Data Mining and Knowledge Discovery*, 34(5):1454–1495, 2020.
- [20] Angus Dempster, Daniel F Schmidt, and Geoffrey I Webb. Minirocket: A very fast (almost) deterministic transform for time series classification. In *Proceedings of the 27th ACM SIGKDD conference on knowledge discovery & data mining*, pages 248–257, 2021.
- [21] Wenjie Du. Pypots: A python toolbox for data mining on partially-observed time series. *arXiv preprint arXiv:2305.18811*, 2023.
- [22] Wenjie Du, David Côté, and Yan Liu. Saits: Self-attention-based imputation for time series. *Expert Systems with Applications*, 219:119619, 2023.
- [23] Iain S Duff, Albert Maurice Erisman, and John Ker Reid. *Direct methods for sparse matrices*. Oxford University Press, 2017.
- [24] Carlos Andres Ferrero, Luis Otavio Alvares, Willian Zalewski, and Vania Bogorny. Movelets: Exploring relevant subtrajectories for robust trajectory classification. In *Proceedings of the 33rd Annual ACM symposium on applied computing*, pages 849–856, 2018.
- [25] Jingkun Gao, Suman Giri, Emre Can Kara, and Mario Berges. PLAID: a public dataset of high-resolution electrical appliance measurements for load identification research: demo abstract. In *BuildSys*, pages 198–199. ACM, 2014.
- [26] Rakshitha Godahewa, Christoph Bergmeir, Geoffrey I Webb, Rob J Hyndman, and Pablo Montero-Manso. Monash time series forecasting archive. *arXiv preprint arXiv:2105.06643*, 2021.
- [27] Ary L Goldberger, Luis AN Amaral, Leon Glass, Jeffrey M Hausdorff, Plamen Ch Ivanov, Roger G Mark, Joseph E Mietus, George B Moody, Chung-Kang Peng, and H Eugene Stanley. Physiobank, physiotoolkit, and physionet: components of a new research resource for complex physiological signals. *circulation*, 101(23):e215–e220, 2000.
- [28] Joze Guna, Grega Jakus, Matevz Pogacnik, Saso Tomazic, and Jaka Sodnik. An analysis of the precision and reliability of the leap motion sensor and its suitability for static and dynamic tracking. *Sensors*, 14(2):3702–3720, 2014.
- [29] Nacereddine Hammami and Mouldi Bedda. Improved tree model for arabic speech recognition. In *2010 3rd international conference on computer science and information technology*, volume 5, pages 521–526. IEEE, 2010.
- [30] Charles R. Harris, K. Jarrod Millman, Stéfan J. van der Walt, Ralf Gommers, Pauli Virtanen, David Cournapeau, Eric Wieser, Julian Taylor, Sebastian Berg, Nathaniel J. Smith, Robert Kern, Matti Picus, Stephan Hoyer, Marten H. van Kerkwijk, Matthew Brett, Allan Haldane, Jaime Fernández del Río, Mark Wiebe, Pearu Peterson, Pierre Gérard-Marchant, Kevin Sheppard, Tyler Reddy, Warren Weckesser, Hameer Abbasi, Christoph Gohlke, and Travis E. Oliphant. Array programming with NumPy. *Nature*, 585(7825):357–362, September 2020.
- [31] Hrayr Harutyunyan, Hrant Khachatrian, David C. Kale, Greg Ver Steeg, and Aram Galstyan. Multitask learning and benchmarking with clinical time series data. *Scientific Data*, 6(1):96, 2019.

- [32] Andrew Harvey, Siem Jan Koopman, and Jeremy Penzer. Messy time series: a unified approach. *Advances in econometrics*, 13:103–144, 1998.
- [33] Stephan Hoyer and Joe Hamman. xarray: Nd labeled arrays and datasets in python. *Journal of Open Research Software*, 5(1):10–10, 2017.
- [34] Alexander Ihler, Jon Hutchins, and Padhraic Smyth. Adaptive event detection with time-varying poisson processes. In *KDD*, pages 207–216. ACM, 2006.
- [35] Abdullah Al Imran, Md Shamsur Rahim, and Tanvir Ahmed. Mining the productivity data of the garment industry. *Int. J. Bus. Intell. Data Min.*, 19(3):319–342, 2021.
- [36] Ali Ismail-Fawaz, Angus Dempster, Chang Wei Tan, Matthieu Herrmann, Lynn Miller, Daniel F Schmidt, Stefano Berretti, Jonathan Weber, Maxime Devanne, Germain Forestier, et al. An approach to multiple comparison benchmark evaluations that is stable under manipulation of the compare set. *arXiv preprint arXiv:2305.11921*, 2023.
- [37] Nathalie Japkowicz. Assessment metrics for imbalanced learning. *Imbalanced learning: Foundations, algorithms, and applications*, pages 187–206, 2013.
- [38] Alistair Johnson, Tom Pollard, and Roger Mark. Mimic-iii clinical database demo (version 1.4). *PhysioNet*, 10:C2HM2Q, 2019.
- [39] Alistair EW Johnson, Tom J Pollard, Lu Shen, Li-wei H Lehman, Mengling Feng, Mohammad Ghassemi, Benjamin Moody, Peter Szolovits, Leo Anthony Celi, and Roger G Mark. Mimic-iii, a freely accessible critical care database. *Scientific data*, 3(1):1–9, 2016.
- [40] Guolin Ke, Qi Meng, Thomas Finley, Taifeng Wang, Wei Chen, Weidong Ma, Qiwei Ye, and Tie-Yan Liu. Lightgbm: A highly efficient gradient boosting decision tree. *Advances in neural information processing systems*, 30, 2017.
- [41] Patrick Kidger. *On Neural Differential Equations*. PhD thesis, University of Oxford, 2021.
- [42] Patrick Kidger, James Morrill, James Foster, and Terry Lyons. Neural controlled differential equations for irregular time series. *Advances in Neural Information Processing Systems*, 33:6696–6707, 2020.
- [43] Tamara G Kolda and Brett W Bader. Tensor decompositions and applications. *SIAM review*, 51(3):455–500, 2009.
- [44] David M Kreindler and Charles J Lumsden. The effects of the irregular sample and missing data in time series analysis. *Nonlinear dynamics, psychology, and life sciences*, 10(2):187–214, 2006.
- [45] Mineichi Kudo, Jun Toyama, and Masaru Shimbo. Multidimensional curve classification using passing-through regions. *Pattern Recognit. Lett.*, 20(11-13):1103–1111, 1999.
- [46] Cristiano Landi, Riccardo Guidotti, Mirco Nanni, and Anna Monreale. The trajectory interval forest classifier for trajectory classification. In *SIGSPATIAL/GIS*, pages 67:1–67:4. ACM, 2023.
- [47] Cristiano Landi, Francesco Spinnato, Riccardo Guidotti, Anna Monreale, and Mirco Nanni. Geolet: An interpretable model for trajectory classification. In *IDA*, volume 13876 of *Lecture Notes in Computer Science*, pages 236–248. Springer, 2023.
- [48] Steven Cheng-Xian Li and Benjamin Marlin. Learning from irregularly-sampled time series: A missing data perspective. In *International Conference on Machine Learning*, pages 5937–5946. PMLR, 2020.
- [49] Zekun Li, Shiyang Li, and Xifeng Yan. Time series as images: Vision transformer for irregularly sampled time series. *Advances in Neural Information Processing Systems*, 36:49187–49204, 2023.
- [50] Jiexi Liu, Meng Cao, and Songcan Chen. Musicnet: A gradual coarse-to-fine framework for irregularly sampled multivariate time series analysis. *arXiv preprint arXiv:2412.01063*, 2024.

- [51] Markus Löning, Anthony Bagnall, Sajaysurya Ganesh, Viktor Kazakov, Jason Lines, and Franz J Király. sktime: A unified interface for machine learning with time series. *arXiv preprint arXiv:1909.07872*, 2019.
- [52] Scott M Lundberg and Su-In Lee. A unified approach to interpreting model predictions. *Advances in neural information processing systems*, 30, 2017.
- [53] Yonghong Luo, Xiangrui Cai, Ying Zhang, Jun Xu, et al. Multivariate time series imputation with generative adversarial networks. *Advances in neural information processing systems*, 31, 2018.
- [54] Antigoni Mezari and Ilias Maglogiannis. An easily customized gesture recognizer for assisted living using commodity mobile devices. *Journal of Healthcare Engineering*, 2018(1):3180652, 2018.
- [55] Matthew Middlehurst, Ali Ismail-Fawaz, Antoine Guillaume, Christopher Holder, David Guijo-Rubio, Guzál Bulatova, Leonidas Tsaprounis, Lukasz Mentel, Martin Walter, Patrick Schäfer, et al. aeon: a python toolkit for learning from time series. *Journal of Machine Learning Research*, 25(289):1–10, 2024.
- [56] Matthew Middlehurst, Patrick Schäfer, and Anthony Bagnall. Bake off redux: a review and experimental evaluation of recent time series classification algorithms. *Data Mining and Knowledge Discovery*, pages 1–74, 2024.
- [57] Robin Mitra, Sarah F McGough, Tapabrata Chakraborti, Chris Holmes, Ryan Copping, Niels Hagenbuch, Stefanie Biedermann, Jack Noonan, Brieuc Lehmann, Aditi Shenvi, et al. Learning from data with structured missingness. *Nature Machine Intelligence*, 5(1):13–23, 2023.
- [58] Luis Moreira-Matias, Michel Ferreira, Joao Mendes-Moreira, L. L., and J. J. Taxi Service Trajectory - Prediction Challenge, ECML PKDD 2015. UCI Machine Learning Repository, 2013. DOI: <https://doi.org/10.24432/C55W25>.
- [59] Adam Paszke, Sam Gross, Soumith Chintala, Gregory Chanan, Edward Yang, Zachary DeVito, Zeming Lin, Alban Desmaison, Luca Antiga, and Adam Lerer. Automatic differentiation in pytorch. 2017.
- [60] Jim Pivarski, Peter Elmer, and David Lange. Awkward arrays in python, c++, and numba. In *EPJ Web of Conferences*, volume 245, page 05023. EDP Sciences, 2020.
- [61] Attila Reiss and Didier Stricker. Introducing a new benchmarked dataset for activity monitoring. In *2012 16th international symposium on wearable computers*, pages 108–109. IEEE, 2012.
- [62] Matthew A Reyna, Christopher S Josef, Russell Jeter, Supreeth P Shashikumar, M Brandon Westover, Shamim Nemati, Gari D Clifford, and Ashish Sharma. Early prediction of sepsis from clinical data: the physionet/computing in cardiology challenge 2019. *Critical care medicine*, 48(2):210–217, 2020.
- [63] Yulia Rubanova, Ricky TQ Chen, and David K Duvenaud. Latent ordinary differential equations for irregularly-sampled time series. *Advances in neural information processing systems*, 32, 2019.
- [64] Donald B Rubin. Inference and missing data. *Biometrika*, 63(3):581–592, 1976.
- [65] Alejandro Pasos Ruiz, Michael Flynn, James Large, Matthew Middlehurst, and Anthony Bagnall. The great multivariate time series classification bake off: a review and experimental evaluation of recent algorithmic advances. *Data Mining and Knowledge Discovery*, 35(2):401–449, 2021.
- [66] Naoki Saito. *Local feature extraction and its applications using a library of bases*. Yale University, 1994.
- [67] Hiroaki Sakoe and Seibi Chiba. Dynamic programming algorithm optimization for spoken word recognition. *IEEE transactions on acoustics, speech, and signal processing*, 26(1):43–49, 1978.

- [68] Md Abu Hanif Shaikh and KM Azharul Hasan. Efficient storage scheme for n-dimensional sparse array: Gcrs/gccs. In *2015 International Conference on High Performance Computing & Simulation (HPCS)*, pages 137–142. IEEE, 2015.
- [69] Satya Narayan Shukla and Benjamin M. Marlin. Multi-time attention networks for irregularly sampled time series. In *9th International Conference on Learning Representations, ICLR 2021, Virtual Event, Austria, May 3-7, 2021*. OpenReview.net, 2021.
- [70] Robert H Shumway, David S Stoffer, and David S Stoffer. *Time series analysis and its applications*, volume 3. Springer, 2000.
- [71] Ikaro Silva, George Moody, Daniel J Scott, Leo A Celi, and Roger G Mark. Predicting in-hospital mortality of icu patients: The physionet/computing in cardiology challenge 2012. In *2012 computing in cardiology*, pages 245–248. IEEE, 2012.
- [72] Francesco Spinnato, Riccardo Guidotti, Anna Monreale, and Mirco Nanni. Fast, interpretable and deterministic time series classification with a bag-of-receptive-fields. *IEEE Access*, 2024.
- [73] Chang Wei Tan, Christoph Bergmeir, Francois Petitjean, and Geoffrey I Webb. Monash university, uea, ucr time series extrinsic regression archive. *arXiv preprint arXiv:2006.10996*, 2020.
- [74] Romain Tavenard, Johann Faouzi, Gilles Vandewiele, Felix Divo, Guillaume Androz, Chester Holtz, Marie Payne, Roman Yurchak, Marc Rußwurm, Kushal Kolar, and Eli Woods. Tslearn, a machine learning toolkit for time series data. *Journal of Machine Learning Research*, 21(118):1–6, 2020.
- [75] Andreas Theissler, Francesco Spinnato, Udo Schlegel, and Riccardo Guidotti. Explainable ai for time series classification: a review, taxonomy and research directions. *Ieee Access*, 10:100700–100724, 2022.
- [76] Leonardo Uieda, Santiago Soler, Rémi Rampin, Hugo van Kemenade, Matthew Turk, Daniel Shapero, Anderson Banihirwe, and John Leeman. Pooch: A friend to fetch your data files. *Journal of Open Source Software*, 5(45):1943, January 2020.
- [77] V Vidulin, M Lustrek, B Kaluza, R Piltaver, and J Krivec. Localization data for person activity. *UCI Machine Learning Repository*, 2010.
- [78] Jun Wang, Wenjie Du, Wei Cao, Keli Zhang, Wenjia Wang, Yuxuan Liang, and Qingsong Wen. Deep learning for multivariate time series imputation: A survey. *arXiv preprint arXiv:2402.04059*, 2024.
- [79] Philip B Weerakody, Kok Wai Wong, Guanjin Wang, and Wendell Ela. A review of irregular time series data handling with gated recurrent neural networks. *Neurocomputing*, 441:161–178, 2021.
- [80] Ben H. Williams, Marc Toussaint, and Amos J. Storkey. Extracting motion primitives from natural handwriting data. In *ICANN (2)*, volume 4132 of *Lecture Notes in Computer Science*, pages 634–643. Springer, 2006.
- [81] Haixu Wu, Tengge Hu, Yong Liu, Hang Zhou, Jianmin Wang, and Mingsheng Long. Timesnet: Temporal 2d-variation modeling for general time series analysis. *arXiv preprint arXiv:2210.02186*, 2022.
- [82] Haixu Wu, Tengge Hu, Yong Liu, Hang Zhou, Jianmin Wang, and Mingsheng Long. Timesnet: Temporal 2d-variation modeling for general time series analysis. In *The Eleventh International Conference on Learning Representations, ICLR 2023, Kigali, Rwanda, May 1-5, 2023*. OpenReview.net, 2023.
- [83] Xiang Zhang, Marko Zeman, Theodoros Tsiligkaridis, and Marinka Zitnik. Graph-guided network for irregularly sampled multivariate time series. In *The Tenth International Conference on Learning Representations, ICLR 2022, Virtual Event, April 25-29, 2022*. OpenReview.net, 2022.



- [84] Liangwei Nathan Zheng, Zhengyang Li, Chang George Dong, Wei Emma Zhang, Lin Yue, Miao Xu, Olaf Maennel, and Weitong Chen. Irregularity-informed time series analysis: Adaptive modelling of spatial and temporal dynamics. In *Proceedings of the 33rd ACM International Conference on Information and Knowledge Management*, pages 3405–3414, 2024.
- [85] Yu Zheng, Quannan Li, Yukun Chen, Xing Xie, and Wei-Ying Ma. Understanding mobility based on GPS data. In *UbiComp*, volume 344 of *ACM International Conference Proceeding Series*, pages 312–321. ACM, 2008.
- [86] Yu Zheng, Xing Xie, and Wei-Ying Ma. Geolife: A collaborative social networking service among user, location and trajectory. *IEEE Data Eng. Bull.*, 33(2):32–39, 2010.
- [87] Yu Zheng, Lizhu Zhang, Xing Xie, and Wei-Ying Ma. Mining interesting locations and travel sequences from gps trajectories. In *Proceedings of the 18th international conference on World wide web*, pages 791–800, 2009.

## A Summary of Notation

We have adopted a tensor-like notation inspired by [43]. The time series dataset is structured along three dimensions: the instance dimension, which consists of  $n$  instances (e.g.,  $X_i$  denotes the  $i$ -th time series in the dataset  $\mathcal{X}$ ); the signal dimension, which includes  $d$  channels (e.g.,  $\mathbf{x}_{i,j}$  represents the  $j$ -th signal in time series  $X_i$ ); and the time dimension, spanning  $\mathcal{T}$  points (e.g.,  $x_{i,j,t_k}$  represents the  $t_k$  observation of  $j$ -th signal in time series  $X_i$ ). We use tildes to specify the index being referenced (e.g.,  $t_k \in \mathbf{t}$  corresponds to the  $k$ -th timestamp at the dataset’s level, while  $t_k \in \tilde{\mathbf{t}}$  corresponds to the  $k$ -th timestamp at the time series’s level). For improved readability, indices are omitted when they are not relevant.

Table 4: Summary of notation.

Notation	
$\mathcal{X}, X, \mathbf{x}, x$	time series dataset, instance, signal, entry
$\mathbf{t}, \tilde{\mathbf{t}}, \tilde{t}, t$	timestamps for a time series dataset, instance, signal, entry
$\mathbf{k}$	timestamp index
$n$	number of instances in a dataset
$d$	number of signals in a time series
$\mathcal{T}, T, \tau$	number timestamps in a time series dataset, instance, signal
$i, j, k$	indexes for instances, signals, timestamps

## B Experimental Details.

In this section, we summarize experimental details regarding the models and datasets, and report further experimental results.

### B.1 Models

The objective of these experiments is to benchmark methods capable of naturally handling irregular time series without introducing bias through imputation techniques. To achieve this, we limit our evaluation to classifiers that inherently support missing data in their input and are available in major time series libraries. Below, we describe the implementation details and hyperparameters for each method. Parameters that are not mentioned are left to their default in their library implementation.

**Bag-of-Receptive-Fields (BORF)** The Bag of Receptive Fields (BORF) algorithm [72] from the `aeon` library extracts discretized subsequences and counts their appearance in the time series, allowing the presence of missing data. A downstream `LightGBM` classifier with default parameters is used to handle transformed features. For the fine-tuned benchmark, the hyperparameter was on performed on the `min_window_to_signal_std_ratio` in the interval  $[0, 0.2]$  with 0.05 increments.

**Bidirectional Recurrent Imputation for Time Series (BRITS)** The BRITS algorithm [9], also from the `pyots` library, employs a bidirectional recurrent network for imputing and classifying incomplete time series. It uses a hidden layer size of 256 and a batch size of 32. Training runs for up to 1000 epochs, with early stopping after 50 epochs of no improvement.

**Gated Recurrent Unit with Decay (GRU-D)** The GRU-D model [11], available in the `pyots` library, extends the Gated Recurrent Unit architecture by introducing decay mechanisms that account for missing data patterns. The recurrent hidden layer size is set to 256, with a batch size of 32. Training uses a maximum of 1000 epochs, with early stopping triggered after 50 epochs of no improvement.

**K-Nearest Neighbors with DTW (KNN)** This baseline model employs the `tslearn` K-Nearest Neighbors algorithm, configured to use the Dynamic Time Warping (DTW) distance measure. DTW incorporates temporal alignment to handle time series of varying lengths effectively. The distance computation uses a Sakoe-Chiba band [67] of 10 points, which limits the warping window to a fixed radius.

**LightGBM (LGBM)** LightGBM [40] is a gradient-boosting framework optimized for speed and efficiency, and can naturally handle missing values. In this baseline, it is trained directly with default parameters on raw time series data transformed into a tabular format using the `sktime` `Tabularizer`. For the fine-tuned benchmark, hyperparameter optimization was conducted over a predefined search space that included the number of leaves ( $num\_leaves$ )  $\in \{31, 63, 127\}$ , maximum tree depth ( $max\_depth$ )  $\in \{-1, 7, 10\}$ , ( $learning\_rate$ )  $\in \{0.05, 0.1\}$ , and the minimum number of samples per leaf ( $min\_data\_in\_leaf$ )  $\in \{20, 100\}$ .

**Neural Controlled Differential Equation (NCDE)** The Neural CDE model [42], implemented via the `diffrax` library, learns continuous-time representations of time series data using differential equations. It employs an Euler solver with a maximum of 100 steps, with step size equal to the minimum time difference between any two adjacent observations, a hidden layer size of 8, and a width size of 32. Training uses a maximum of 1000 iterations, using Adam as optimizer, with a starting learning rate of 0.01, patience of 200 for early stopping, and a learning rate reduction factor of 0.5 after 50 stagnant iterations.

**Raindrop (RAINDROP)** The Raindrop model [83], a graph-based neural network from `pypots`, handles irregular time series by sending messages over graphs that are optimized for capturing time-varying dependencies among sensors. This model uses 2 layers, a feed-forward network size of 256, 2 attention heads, and a dropout rate of 0.3. Training employs a batch size of 32, with early stopping after 50 epochs of no improvement.

**Random Interval Feature Classifier (RIFC)** The Random Interval Feature Classifier (RIFC) leverages the `RandomIntervalFeatureExtractor` from the `sktime` library to generate simple statistical summaries (mean, standard deviation, minimum, maximum, median, skewness, and kurtosis) from randomly selected intervals within the time series, with the number of intervals being the logarithm of the time series length. These features are subsequently used by a downstream LightGBM classifier to perform classification.

**Minimally Random Convolutional Kernel Transform (ROCKET)** Rocket, in its `Minirocket` implementation [20] from the `sktime` library, employs 10000 fixed convolutional kernels to extract features from time series data. This implementation includes `MiniRocketMultivariateVariable`, which handles multivariate time series while tolerating missing data. The transformation could include missing data; therefore, instead of the most common ridge classifier, LightGBM with default parameters is used. For the fine-tuned benchmark, hyperparameter optimization was conducted over the number of kernels,  $num\_kernels \in \{100, 500, 1000, 5000, 10000, 50000\}$ .

**Self-Attention Imputation for Time Series (SAITS)** The SAITS model [22], implemented in the `pypots` library, employs a transformer-based architecture specifically tailored for time series imputation. It utilizes a dual self-attention mechanism across temporal dimensions, enabling it to capture both global and local patterns despite missing values. In this configuration, SAITS is trained with 2 attention layers, a model dimension of 256, 4 attention heads, and hidden dimensions  $d_k = 64$ ,  $d_v = 64$ , and  $d_{ffn} = 128$ . A dropout rate of 0.1 is used for both the transformer blocks and attention layers. The model is optimized over a maximum of 1000 epochs, with early stopping triggered after 50 stagnant epochs. Training is performed with a batch size of 32.

**Support Vector Machine with LCSS Kernel (SVM)** This method uses the `sktime` implementation of a Support Vector Machine, enhanced with the Longest Common Subsequence (LCSS) distance kernel [4]. LCSS is robust to missing values and temporal distortions, as it matches time series subsequences with allowable gaps. The kernel uses a Sakoe-Chiba constraint with a radius of 10. Each time series is standardized using z-score normalization. The model is trained for a maximum of 1000 iterations.

**TimesNet (TIMESNET)** TimesNet [82] is a modern transformer-based architecture designed for multivariate time series modeling, emphasizing temporal receptive fields through learnable convolutional kernels. Its implementation here leverages 2 layers and 3 convolutional kernels with dynamic top- $k$  temporal selection. The model dimension is set to 64, with a feed-forward network size of 128. Training is conducted using a batch size of 32 over 1000 epochs, with early stopping after 50 epochs without validation improvement.

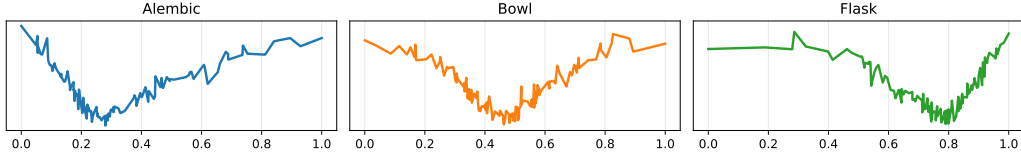


Figure 9: Three examples of instances from the (ABF) dataset, from left to right, Alembic, Bowl, and Flask.

## B.2 Datasets

The repository includes 34 datasets, each briefly described below, along with the data preparation steps applied.<sup>3</sup> For datasets without a predefined train-test split, we created a stratified, instance-based 70-30% train-test split.

**Alembics Bowls Flasks. (ABF)** This dataset is inspired by the classical Cylinder-Bell-Funnel (CBF) benchmark [66] for regular time series classification. Similarly to CBF, there are three classes, which are Alembics, Bowls, and Flasks. The classes differ by how much the temporal axis is skewed, i.e., if it has positive (Alembic), negative (Flask), or no skewness (Bowl). For each time series, 128 values are sampled from a circumference and then standardized. There are 10 instances for each class in the training set and 300 for each in the test set. An example is presented in Figure 9.

**Animals (AN)** This dataset, generated during the Starkey project [24], consists of trajectories from three animal species—elk, deer, and cattle. The classification task commonly used in the literature [24, 47, 46] involves inferring the species based on movement patterns. The target classes in the dataset are balanced, with 38 trajectories for the elk, 30 for the deer, and 34 for the cattle.

**Geolife (GS)** This dataset was collected during the GeoLife Project (Microsoft Research Asia) from April 2007 to August 2012 [87, 85, 86]. It contains the trajectories of 182 users and has been preprocessed as detailed in the *User Guide-1*.<sup>4</sup> One of the most common supervised machine-learning tasks using this dataset is to identify (a subset) of the 11 means of transportation. We defined three target variables with a decreasing number of classes. The first target variable includes all the means of transportation in the dataset: airplane, bike, boat, bus, car, motorcycle, run, subway, taxi, train, and walk. The second target variable, used in [24], groups the transportation modes into six classes: bike, bus/taxi, car, subway, train, and walk. The third target variable, used in [47], simplifies the classification into two categories: private (bike, boat, car, motorcycle, run, walk) and public (the remaining modes of transportation). In Section 5, we benchmark the models against the first target variable. In this setting, each class accounts for approximately 9.1% of the total instances, but the standard deviation is 12.7%, i.e., the target variable is highly imbalanced.

**GPS Data of Seabirds (SE)** This dataset, introduced in [8], consists of GPS data collected from 108 seabirds spanning three species: European shag (15), common guillemot (31), and razorbill (62). Similar to the *Animals* dataset, the species has been used to evaluate model performance in inferring species. The target variable is imbalanced, with the majority class (razorbill) comprising 62 individuals, while the minority class (European shag) includes only 15.

**Localization Data for Person Activity (LPA)** Introduced in [77], this dataset contains data from 5 individuals performing 11 different actions: falling, lying, lying down, on all fours, sitting, sitting down, sitting on the ground, standing up from lying, standing up from sitting, standing up from sitting on the ground, walking. Each action was recorded by tracking the positions of the body’s right and left ankles, chest, and belt in a 3-dimensional space, resulting in 12 distinct signals per time series.

**MIMIC-III Clinical Database Demo (MI3)** Introduced by [39, 38] on the Physionet platform [27], the dataset contains health-related data associated with 40,000 patients in critical care at the

<sup>3</sup>Data is hosted at <https://huggingface.co/datasets/splandi/pyrregular>.

<sup>4</sup>The user guide is included in the zip folder containing the data, which is available for download directly from Microsoft at [t.ly/blDnH](https://t.ly/blDnH).

Beth Israel Deaconess Medical Center from 2001 to 2012. Since the full version is available to credentialed users under strict requirements, we use the publicly available demo version in our work. We preprocess the data in accordance with [31]. The classification target involves predicting in-hospital mortality.

**PAMAP2 Physical Activity Monitoring (PA2)** This dataset, introduced in [61], contains data from 9 subjects (1 female, 8 male) performing 19 different physical activities: ascending stairs, car driving, computer work, cycling, descending stairs, folding laundry, house cleaning, ironing, lying, nordic walking, playing soccer, rope jumping, running, sitting, standing, transient, vacuum cleaning, walking, watching TV. The data includes measurements from 3 inertial measurement units (IMUs) positioned on the dominant arm, chest, and dominant side’s ankle. Specifically, from each IMU sensor, the dataset contains information about the temperature, the 3-dimensional acceleration, gyroscope and magnetometer data, and the sensor orientation. Additionally, heart rate observations are included. The two types of sensors record data at different sampling rates: 100 Hz for the IMUs and 9 Hz for the heart rate monitor. We preprocess the data according to the authors’ guidelines when downloading the dataset. Data from the “transient” activity, i.e., movements between the end of one activity and the start of another, was excluded. The remaining 18 activities serve as classification target classes.

**PhysioNet 2012 (P12)** Published as data for the “Predicting Mortality of ICU Patients: The PhysioNet/Computing in Cardiology” challenge in 2012 [71], the data contains information about the patient, like age, gender, height, and weight, and 37 different types of time series. Similar to the MIMIC-III dataset, the classification target is about predicting in-hospital death.

**PhysioNet 2019 (P19)** Published as data for the “Early Prediction of Sepsis from Clinical Data: The PhysioNet/Computing in Cardiology” challenge in 2019 [62], the dataset contains demographic information about the patients, such as age, gender, height, and weight, alongside 34 other time-series variables for vital signs and laboratory test values. The classification task involves predicting whether a patient has sepsis or not.

**Productivity Prediction of Garment Employees (PGE)** Introduced in [35], this dataset contains information about garment manufacturing processing on a per-team level. Additionally, this dataset contains a team productivity performance index, which ranges between 0 and 1. As suggested by the authors, we use this index as a classification target. Specifically, we defined a team *efficient* if the productivity performance index is strictly greater than 0.75.

**Taxi (TA)** This dataset, introduced as part of the “ECML/PKDD 15: Taxi Trip Time Prediction (II) Competition” [58] consists of 121,312 trajectories of Taxis in Porto (Portugal). The classification task is to predict the type of call that generated the run. The types of calls could be: *A* if this trip was dispatched from the central, *B* if this trip was demanded directly to a taxi driver on a specific stand *C* otherwise. The classes are balanced.

**Vehicles (VE)** GPS trajectories about two different types of vehicles -buses and trucks- moving in Athens. This dataset is available from download from the ChoroChronos Archive<sup>5</sup>.

**UEA and UCR Irregular Datasets.** The other 22 irregular time-series datasets were downloaded from the UEA and UCR dataset repository<sup>6</sup> [17, 5]. In particular, we included the following datasets:

- 11 variable-length univariate time series classification problems from [6]: AllGestureWiimoteX, AllGestureWiimoteY and AllGestureWiimoteZ (GX, GY, GZ) from [28]; GestureMidAirD1, GestureMidAirD2, and GestureMidAirD3 (GM1, GM2, GM3) from [10]; GesturePebbleZ1 and GesturePebbleZ2 (GP1, GP2) from [54]; PickupGestureWiimoteZ and ShakeGestureWiimoteZ (PGZ, SGZ) from [28]; PLAID (PL) from [25];
- 4 fixed length univariate time series with missing values from [56]: DodgerLoopDay, DodgerLoopGame, and DodgerLoopWeekend (DD, DG, DW) from [34]; MelbournePedestrian (MP) [15] extracted from the City of Melbourne website;

---

<sup>5</sup>chorochronos.org

<sup>6</sup>timeseriesclassification.com

Table 5: Summary of dataset characteristics: the number of instances (#Inst), signals (#Sign), and observations (#Obs); target classes (#TC) and class imbalance (CU); as well as time-series-specific metrics like missing values (MV) and sampling coefficient of variation (SCV), and each type of irregularity, i.e., unevenly sampled (US), partially observed (PO), unequal length (UL), shift (SH), ragged sampling (RS).

Cat	Name	Source	#Inst	#Sign	#Obs	#TC	CU ( $\sigma$ )	MV (%)	SVC	US	PO	UL	SH	RS
<i>health</i>	MI3	[39]	57	17	145	2	0.20	0.83	0.60	✓	✓	✓	✓	✓
	P12	[71]	7990	37	203	2	0.36	0.94	0.59	✓	✓	✓	✓	✓
	P19	[62]	40334	34	334	2	0.43	0.98	0.18	✓	✓	✓	✓	✓
<i>human activity recognition</i>	CT	[80]	2858	3	182	20	0.01	0.34	0.00	✗	✗	✓	✗	✗
	GM1	[10]	338	1	360	26	0.00	0.54	0.00	✗	✗	✓	✗	✗
	GM2	[10]	338	1	360	26	0.00	0.54	0.00	✗	✗	✓	✗	✗
	GM3	[10]	338	1	360	26	0.00	0.54	0.00	✗	✗	✓	✗	✗
	GP1	[54]	304	1	455	6	0.01	0.52	0.00	✗	✗	✓	✗	✗
	GP2	[54]	304	1	455	6	0.01	0.52	0.00	✗	✗	✓	✗	✗
	GX	[28]	1000	1	385	10	0.00	0.68	0.00	✗	✗	✓	✗	✗
	GY	[28]	1000	1	385	10	0.00	0.68	0.00	✗	✗	✓	✗	✗
	GZ	[28]	1000	1	385	10	0.00	0.68	0.00	✗	✗	✓	✗	✗
	LPA	[77]	273	12	2870	11	0.00	0.95	9.04	✓	✗	✓	✓	✓
	PAM	[61]	124	52	110883	16	0.03	0.82	0.01	✓	✓	✓	✓	✓
	PGZ	[28]	100	1	361	10	0.00	0.60	0.00	✗	✗	✓	✗	✗
	SGZ	[28]	100	1	385	10	0.00	0.57	0.00	✗	✗	✓	✗	✗
<i>mobility</i>	AN	[24]	102	2	291	3	0.03	0.50	1.21	✓	✗	✓	✗	✓
	AOC	[18]	781	3	736	4	0.03	0.59	0.00	✗	✗	✓	✗	✗
	APT	[18]	2111	3	2371	3	0.06	0.83	0.00	✗	✗	✓	✗	✗
	ARC	[18]	1502	3	4201	2	0.01	0.91	0.00	✗	✗	✓	✗	✗
	GS	[86]	5977	2	96282	11	0.13	0.99	10.27	✓	✗	✓	✓	✓
	MP	[15]	3633	1	24	10	0.00	0.00	0.01	✗	✗	✓	✗	✗
	SE	[8]	108	4	6048	3	0.18	0.60	0.00	✓	✗	✓	✓	✓
	TA	[58]	121312	2	119	3	0.13	0.61	0.00	✓	✗	✓	✓	✓
	VE	[14]	381	2	1095	2	0.22	0.57	5.29	✓	✗	✓	✗	✓
<i>sensor</i>	DD	[34]	158	1	288	7	0.01	0.01	0.00	✗	✓	✗	✗	✗
	DG	[34]	158	1	288	2	0.02	0.01	0.00	✗	✓	✗	✗	✗
	DW	[34]	158	1	288	2	0.21	0.01	0.00	✗	✓	✗	✗	✗
<i>other</i>	IW	[12]	50000	200	22	10	0.00	0.70	0.00	✗	✗	✓	✗	✗
	JV	[45]	640	12	29	9	0.03	0.46	0.00	✗	✗	✓	✗	✗
	PGE	[35]	24	9	59	2	0.13	0.19	0.68	✓	✗	✓	✓	✓
	PL	[25]	1074	1	1344	11	0.05	0.76	0.00	✗	✗	✓	✗	✗
	SAD	[29]	8798	13	93	10	0.00	0.57	0.00	✗	✗	✓	✗	✗
<i>synth</i>	ABF	<i>new!</i>	930	1	128	3	0.00	0.00	1.95	✓	✗	✗	✗	✗

- 7 variable-length multivariate time series from [65]: AsphaltObstaclesCoordinates, Asphalt-PavementTypeCoordinates, and AsphaltRegularityCoordinates (AOC, APT, ARC) from [18]; CharacterTrajectories (CT) from [80]; InsectWingbeat (IW) from [12]; JapaneseVowels (JV) from [45]; SpokenArabicDigits (SAD) from [29];

Table 5 contains the full list of curated datasets at the moment of publication on our repository. The list additionally contains some information about the datasets: the number of instances, #Inst, number of signals, #Sign, and number of observations, #Obs ( $\max_i^n(T_i)$ ), the number of target classes #TC and the standard deviation between the number of instances per class (CU). Additionally, the dataset contains information about the time series, like the percentage of missing values (MV)-computed as the ratio between the *NaN* observations divided by the total number of observations- and the sampling coefficient of variation (SCV), alongside information on the different kind of irregularity in the dataset.

Given  $\mathbf{y}_h$  as the labels vector containing only the  $h$ -th class, CU is defined as follows:

$$CU = \sqrt{\frac{\sum_{h=0}^c (y_h - \mu)^2}{c}} \quad (1)$$



where  $\mu$  is the average number of observations. Given  $\Delta\tilde{t}$  as the vector of differences between consecutive timestamps of a signal, the SCV is computed as the coefficient of variation (the ratio of the standard deviation to the mean) for each signal, averaged first across each time series and then over the entire dataset.

We divided the dataset into 6 categories based on the type of phenomena captured: *healthcare*, *human activity recognition*, *mobility* (or more generically, geo-temporal motion), *sensors*, *synthetic* data, and *others* for datasets that don't fall in any of the previous categories (like the UCR audio and speech categories).

## C Detailed Results

The full result table in terms of F1 and total runtime are available in Tables 6 and 7. Further, we also provide the CD-plots for other common performance metrics (*accuracy*, *roc-auc*, *precision* and *recall*) in Figure 10, as well as CD-plots for subsets of datasets with specific characteristics (Figure 11). While the widely used CD-plot is effective, it has been criticized in [36] for its susceptibility to manipulation, as the average rank of a model can be influenced by the performance of other comparators. For this reason, we also propose MCM matrix for several metrics in Figures 12 to 14. However, in our case, results are consistent with those presented in the main text, and are presented in the appendix due to space limitations. We also report in Figures 15 to 19 the performance using several metrics, different dataset subsets, and against training and inference times.

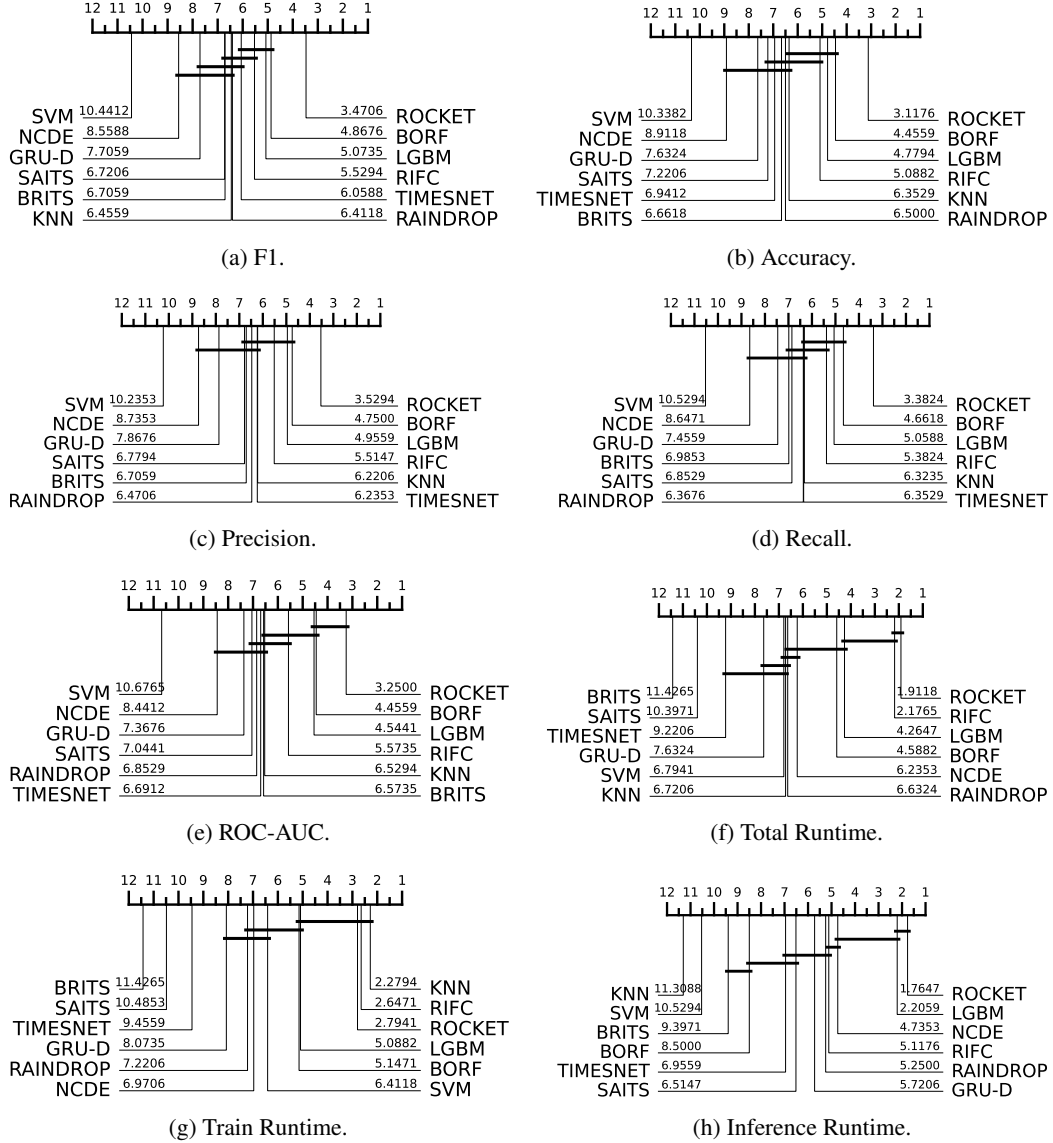


Figure 10: Critical Difference plot for the benchmarked models in terms of different metrics, for all datasets. Best models to the right. The performance of models connected by the bar is statistically tied, using a one-sided Holm-corrected Wilcoxon sign rank test with a critical value of 0.05.

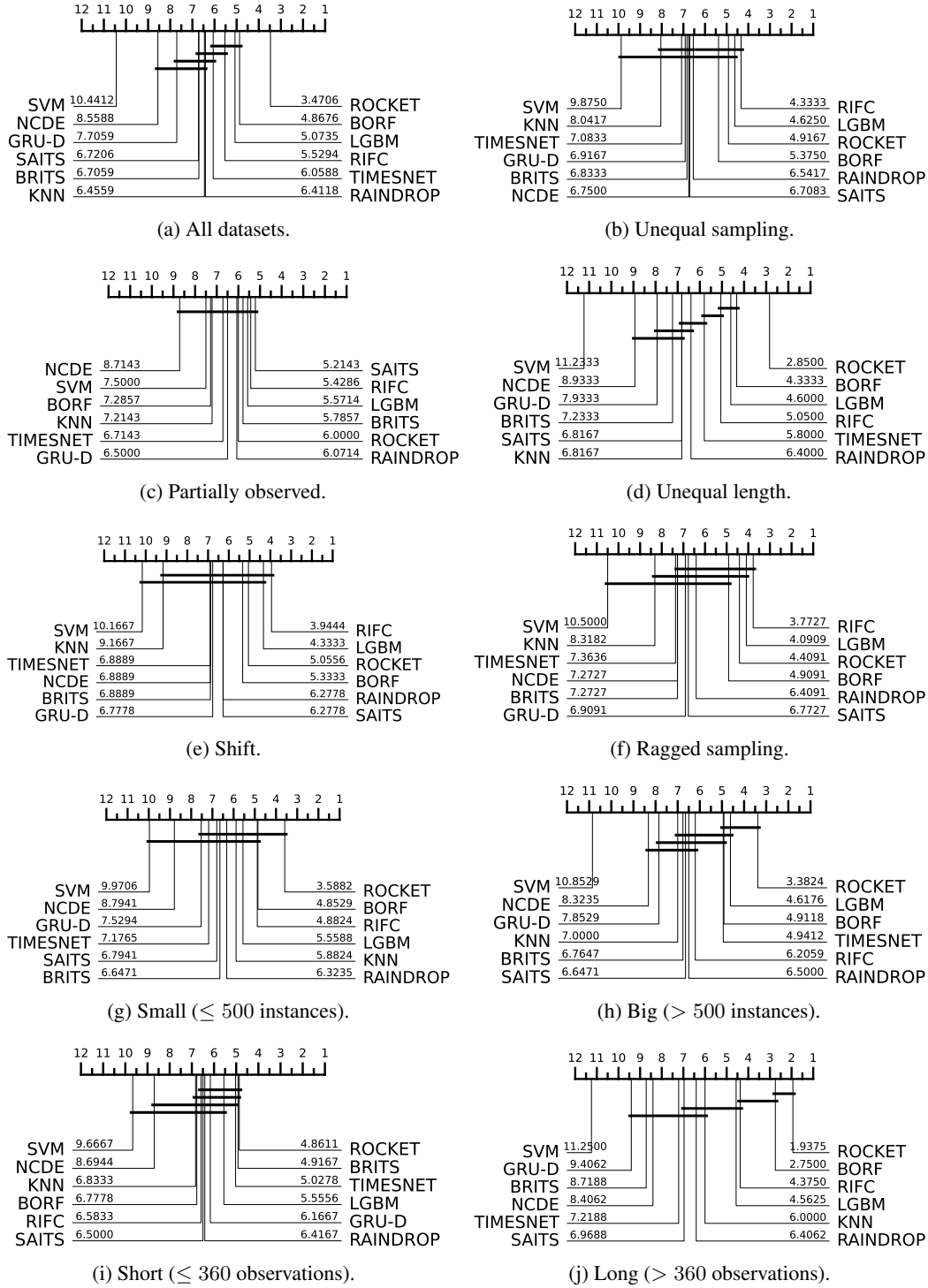


Figure 11: Critical Difference plot for the benchmarked models in terms of F1, divided into different groups. Best models to the right. The performance of models connected by the bar is statistically tied, using a one-sided Holm-corrected Wilcoxon sign rank test with a critical value of 0.05.

	ROCKET 0.669	BORF 0.625	LGBM 0.606	RFC 0.571	TIMESNET 0.525	RAINDROP 0.520	SAITS 0.518	KNN 0.507	BRITS 0.482	GRU-D 0.435	NCDE 0.396	SVM 0.245
Mean-f1												
ROCKET 0.669	Mean-Difference f1c / f1c / f1c Wilcoxon p-value	<b>0.044</b> <b>24 / 3 / 7</b> <b>0.001</b>	<b>0.063</b> <b>24 / 3 / 7</b> <b>0.003</b>	<b>0.098</b> <b>26 / 4 / 4</b> <b>≤ 1e-03</b>	<b>0.144</b> <b>24 / 0 / 10</b> <b>≤ 1e-03</b>	<b>0.149</b> <b>26 / 0 / 8</b> <b>≤ 1e-03</b>	<b>0.151</b> <b>25 / 0 / 9</b> <b>0.001</b>	<b>0.162</b> <b>28 / 0 / 6</b> <b>≤ 1e-03</b>	<b>0.187</b> <b>25 / 0 / 9</b> <b>0.001</b>	<b>0.234</b> <b>25 / 0 / 9</b> <b>≤ 1e-03</b>	<b>0.273</b> <b>27 / 0 / 7</b> <b>≤ 1e-03</b>	<b>0.424</b> <b>31 / 0 / 3</b> <b>≤ 1e-03</b>
BORF 0.625	-0.044 7 / 3 / 24 0.999	-	0.019 19 / 4 / 11 0.084	<b>0.054</b> <b>22 / 3 / 9</b> <b>0.015</b>	<b>0.100</b> <b>20 / 0 / 14</b> <b>0.008</b>	<b>0.105</b> <b>25 / 0 / 9</b> <b>0.002</b>	<b>0.107</b> <b>23 / 0 / 11</b> <b>0.009</b>	<b>0.118</b> <b>20 / 0 / 14</b> <b>0.024</b>	<b>0.143</b> <b>23 / 0 / 13</b> <b>0.006</b>	<b>0.190</b> <b>21 / 0 / 11</b> <b>0.001</b>	<b>0.229</b> <b>28 / 0 / 6</b> <b>≤ 1e-03</b>	<b>0.380</b> <b>29 / 1 / 4</b> <b>≤ 1e-03</b>
LGBM 0.606	-0.063 7 / 3 / 24 0.997	-0.019 11 / 4 / 19 0.916	-	0.035 18 / 3 / 13 0.114	<b>0.081</b> <b>20 / 0 / 14</b> <b>0.007</b>	<b>0.086</b> <b>23 / 0 / 11</b> <b>0.002</b>	<b>0.088</b> <b>23 / 0 / 11</b> <b>0.008</b>	0.099 21 / 0 / 13 0.054	<b>0.124</b> <b>23 / 0 / 11</b> <b>0.003</b>	<b>0.170</b> <b>25 / 0 / 9</b> <b>≤ 1e-03</b>	<b>0.210</b> <b>29 / 0 / 5</b> <b>≤ 1e-03</b>	<b>0.361</b> <b>30 / 1 / 3</b> <b>≤ 1e-03</b>
RFC 0.571	-0.098 4 / 4 / 26 1.000	-0.054 9 / 3 / 22 0.985	-0.035 13 / 3 / 18 0.886	-	0.046 20 / 0 / 14 0.114	<b>0.051</b> <b>21 / 0 / 13</b> <b>0.035</b>	<b>0.053</b> <b>22 / 0 / 12</b> <b>0.039</b>	0.064 21 / 0 / 13 0.098	<b>0.089</b> <b>23 / 0 / 11</b> <b>0.019</b>	<b>0.136</b> <b>25 / 0 / 9</b> <b>0.002</b>	<b>0.175</b> <b>26 / 0 / 8</b> <b>≤ 1e-03</b>	<b>0.326</b> <b>31 / 0 / 3</b> <b>≤ 1e-03</b>
TIMESNET 0.525	-0.144 10 / 0 / 24 1.000	-0.100 14 / 0 / 20 0.992	-0.081 14 / 0 / 20 0.994	-0.046 14 / 0 / 20 0.889	-	0.005 16 / 2 / 16 0.634	0.007 19 / 2 / 13 0.316	0.018 15 / 2 / 17 0.575	0.043 20 / 3 / 11 0.053	<b>0.090</b> <b>23 / 2 / 9</b> <b>0.004</b>	<b>0.129</b> <b>23 / 1 / 10</b> <b>0.001</b>	<b>0.280</b> <b>27 / 2 / 5</b> <b>≤ 1e-03</b>
RAINDROP 0.520	-0.149 8 / 0 / 26 1.000	-0.105 9 / 0 / 25 0.998	-0.086 11 / 0 / 23 0.998	-0.051 13 / 0 / 21 0.967	-0.005 16 / 2 / 16 0.366	-	0.002 20 / 2 / 12 0.269	0.013 16 / 2 / 16 0.152	0.038 26 / 2 / 16 0.595	<b>0.085</b> <b>20 / 2 / 12</b> <b>0.014</b>	<b>0.124</b> <b>26 / 1 / 7</b> <b>≤ 1e-03</b>	<b>0.275</b> <b>28 / 3 / 3</b> <b>≤ 1e-03</b>
SAITS 0.518	-0.151 9 / 0 / 25 0.999	-0.107 11 / 0 / 23 0.992	-0.088 11 / 0 / 23 0.992	-0.053 12 / 0 / 22 0.962	-0.007 13 / 2 / 19 0.684	-0.002 12 / 2 / 20 0.731	-	0.011 17 / 2 / 15 0.714	0.036 20 / 2 / 12 0.196	<b>0.082</b> <b>20 / 2 / 12</b> <b>0.022</b>	<b>0.122</b> <b>27 / 1 / 6</b> <b>≤ 1e-03</b>	<b>0.273</b> <b>29 / 2 / 3</b> <b>≤ 1e-03</b>
KNN 0.507	-0.162 6 / 0 / 28 1.000	-0.118 14 / 0 / 20 0.977	-0.099 13 / 0 / 21 0.948	-0.064 13 / 0 / 21 0.905	-0.018 17 / 2 / 15 0.425	-0.013 16 / 2 / 16 0.405	-0.011 20 / 2 / 12 0.286	-	0.025 14 / 3 / 17 0.422	0.071 18 / 3 / 13 0.101	<b>0.111</b> <b>23 / 2 / 9</b> <b>0.016</b>	<b>0.262</b> <b>25 / 5 / 4</b> <b>≤ 1e-03</b>
BRITS 0.482	-0.187 9 / 0 / 25 0.999	-0.143 11 / 0 / 23 0.994	-0.124 11 / 0 / 23 0.997	-0.089 11 / 0 / 23 0.982	-0.043 11 / 3 / 20 0.947	-0.038 16 / 2 / 16 0.848	-0.036 15 / 2 / 17 0.804	-0.025 17 / 3 / 14 0.578	-	<b>0.047</b> <b>19 / 4 / 11</b> <b>0.004</b>	<b>0.086</b> <b>22 / 1 / 11</b> <b>0.004</b>	<b>0.237</b> <b>27 / 3 / 4</b> <b>≤ 1e-03</b>
GRU-D 0.435	-0.234 9 / 0 / 25 1.000	-0.190 11 / 0 / 23 1.000	-0.170 9 / 0 / 25 1.000	-0.136 9 / 0 / 25 1.000	-0.090 9 / 2 / 23 0.996	-0.085 12 / 2 / 20 0.986	-0.082 12 / 2 / 20 0.989	-0.071 13 / 3 / 18 0.968	-0.047 11 / 4 / 19 0.984	-	0.039 16 / 1 / 17 0.182	<b>0.190</b> <b>27 / 2 / 5</b> <b>≤ 1e-03</b>
NCDE 0.396	-0.273 7 / 0 / 27 1.000	-0.229 6 / 0 / 28 1.000	-0.210 5 / 0 / 29 1.000	-0.175 8 / 0 / 26 1.000	-0.129 10 / 1 / 23 0.999	-0.124 7 / 1 / 26 1.000	-0.122 6 / 1 / 22 1.000	-0.111 9 / 2 / 23 0.984	-0.086 11 / 1 / 22 0.996	-0.039 17 / 1 / 16 0.818	-	<b>0.151</b> <b>27 / 1 / 6</b> <b>≤ 1e-03</b>
SVM 0.245	-0.424 3 / 0 / 31 1.000	-0.380 4 / 1 / 29 1.000	-0.361 3 / 1 / 30 1.000	-0.326 3 / 0 / 31 1.000	-0.280 5 / 2 / 27 1.000	-0.275 3 / 3 / 28 1.000	-0.273 3 / 2 / 29 1.000	-0.262 4 / 5 / 25 1.000	-0.237 4 / 3 / 27 1.000	-0.190 5 / 2 / 27 1.000	-0.151 6 / 1 / 27 1.000	If in bold, then p-value < 0.05

(a) F1 score.

	ROCKET 0.742	BORF 0.700	LGBM 0.674	RFC 0.644	RAINDROP 0.581	TIMESNET 0.576	SAITS 0.568	BRITS 0.554	KNN 0.542	GRU-D 0.508	NCDE 0.456	SVM 0.300
Mean-accuracy												
ROCKET 0.742	Mean-Difference acc / acc / acc Wilcoxon p-value	<b>0.042</b> <b>24 / 3 / 7</b> <b>0.001</b>	<b>0.068</b> <b>25 / 3 / 6</b> <b>0.001</b>	<b>0.098</b> <b>25 / 4 / 5</b> <b>≤ 1e-03</b>	<b>0.161</b> <b>29 / 0 / 5</b> <b>≤ 1e-03</b>	<b>0.166</b> <b>29 / 0 / 5</b> <b>≤ 1e-03</b>	<b>0.174</b> <b>28 / 0 / 6</b> <b>≤ 1e-03</b>	<b>0.188</b> <b>25 / 0 / 9</b> <b>≤ 1e-03</b>	<b>0.200</b> <b>27 / 1 / 6</b> <b>≤ 1e-03</b>	<b>0.234</b> <b>25 / 1 / 8</b> <b>≤ 1e-03</b>	<b>0.286</b> <b>29 / 0 / 5</b> <b>≤ 1e-03</b>	<b>0.442</b> <b>29 / 2 / 3</b> <b>≤ 1e-03</b>
BORF 0.700	-0.042 7 / 3 / 24 0.999	-	0.026 18 / 7 / 9 0.052	<b>0.056</b> <b>21 / 3 / 10</b> <b>0.012</b>	<b>0.119</b> <b>25 / 0 / 9</b> <b>≤ 1e-03</b>	<b>0.124</b> <b>26 / 0 / 8</b> <b>0.001</b>	<b>0.132</b> <b>25 / 0 / 9</b> <b>0.001</b>	<b>0.146</b> <b>21 / 0 / 13</b> <b>0.008</b>	<b>0.158</b> <b>20 / 1 / 13</b> <b>0.014</b>	<b>0.192</b> <b>25 / 0 / 9</b> <b>≤ 1e-03</b>	<b>0.244</b> <b>31 / 0 / 3</b> <b>≤ 1e-03</b>	<b>0.400</b> <b>30 / 1 / 3</b> <b>≤ 1e-03</b>
LGBM 0.674	-0.068 6 / 0 / 28 0.999	-0.026 9 / 7 / 18 0.948	-	0.030 19 / 3 / 12 0.098	<b>0.094</b> <b>25 / 0 / 9</b> <b>≤ 1e-03</b>	<b>0.098</b> <b>25 / 0 / 9</b> <b>≤ 1e-03</b>	<b>0.106</b> <b>24 / 0 / 10</b> <b>0.001</b>	<b>0.120</b> <b>24 / 0 / 10</b> <b>0.001</b>	<b>0.132</b> <b>20 / 1 / 13</b> <b>0.041</b>	<b>0.166</b> <b>26 / 0 / 8</b> <b>≤ 1e-03</b>	<b>0.218</b> <b>30 / 0 / 4</b> <b>≤ 1e-03</b>	<b>0.375</b> <b>30 / 1 / 3</b> <b>≤ 1e-03</b>
RFC 0.644	-0.098 5 / 4 / 25 1.000	-0.056 10 / 3 / 21 0.988	-0.030 12 / 3 / 19 0.902	-	<b>0.064</b> <b>24 / 0 / 10</b> <b>0.012</b>	<b>0.069</b> <b>25 / 0 / 9</b> <b>0.007</b>	<b>0.076</b> <b>24 / 1 / 10</b> <b>0.005</b>	<b>0.091</b> <b>24 / 0 / 10</b> <b>0.011</b>	<b>0.103</b> <b>21 / 0 / 13</b> <b>0.045</b>	<b>0.137</b> <b>26 / 0 / 8</b> <b>≤ 1e-03</b>	<b>0.188</b> <b>31 / 1 / 2</b> <b>≤ 1e-03</b>	<b>0.345</b> <b>27 / 0 / 7</b> <b>≤ 1e-03</b>
RAINDROP 0.581	-0.161 5 / 0 / 29 1.000	-0.119 9 / 0 / 25 1.000	-0.094 9 / 0 / 25 1.000	-0.064 10 / 0 / 24 0.988	-	0.005 18 / 2 / 14 0.252	0.012 21 / 2 / 11 0.114	0.027 18 / 2 / 14 0.537	0.039 15 / 3 / 16 0.537	<b>0.073</b> <b>20 / 2 / 12</b> <b>0.021</b>	<b>0.124</b> <b>28 / 1 / 5</b> <b>≤ 1e-03</b>	<b>0.281</b> <b>27 / 2 / 5</b> <b>≤ 1e-03</b>
TIMESNET 0.576	-0.166 5 / 0 / 29 1.000	-0.124 8 / 0 / 26 0.999	-0.098 9 / 0 / 25 1.000	-0.069 9 / 0 / 25 0.994	-0.005 14 / 2 / 18 0.748	-	0.007 18 / 4 / 12 0.255	0.022 17 / 4 / 13 0.198	0.034 14 / 2 / 18 0.614	<b>0.068</b> <b>22 / 2 / 10</b> <b>0.016</b>	<b>0.120</b> <b>22 / 2 / 10</b> <b>0.002</b>	<b>0.276</b> <b>25 / 2 / 7</b> <b>≤ 1e-03</b>
SAITS 0.568	-0.174 6 / 0 / 28 1.000	-0.132 9 / 0 / 25 0.999	-0.106 10 / 0 / 24 0.995	-0.076 9 / 1 / 24 0.995	-0.012 11 / 2 / 21 0.886	-0.007 12 / 4 / 18 0.745	-	0.015 14 / 3 / 17 0.591	0.027 12 / 2 / 20 0.684	0.061 18 / 2 / 14 0.071	<b>0.112</b> <b>25 / 1 / 8</b> <b>0.001</b>	<b>0.269</b> <b>28 / 2 / 4</b> <b>≤ 1e-03</b>
BRITS 0.554	-0.188 9 / 0 / 25 1.000	-0.146 13 / 0 / 21 0.992	-0.120 10 / 0 / 24 0.999	-0.091 10 / 0 / 24 0.989	-0.027 14 / 2 / 18 0.774	-0.022 13 / 4 / 17 0.802	-0.015 17 / 3 / 14 0.409	-	0.012 16 / 3 / 15 0.510	<b>0.046</b> <b>19 / 4 / 11</b> <b>0.023</b>	<b>0.098</b> <b>22 / 2 / 10</b> <b>0.004</b>	<b>0.254</b> <b>28 / 3 / 3</b> <b>≤ 1e-03</b>
KNN 0.542	-0.200 6 / 1 / 27 1.000	-0.158 13 / 1 / 20 0.986	-0.132 13 / 1 / 20 0.959	-0.103 13 / 0 / 21 0.956	-0.039 16 / 3 / 15 0.463	-0.034 18 / 2 / 14 0.316	-0.027 20 / 2 / 12 0.490	-0.012 15 / 3 / 16 0.490	-	0.034 17 / 4 / 13 0.158	<b>0.086</b> <b>23 / 2 / 9</b> <b>0.028</b>	<b>0.242</b> <b>26 / 5 / 3</b> <b>≤ 1e-03</b>
GRU-D 0.508	-0.234 8 / 1 / 25 1.000	-0.192 9 / 0 / 25 1.000	-0.166 8 / 0 / 26 1.000	-0.137 8 / 0 / 26 1.000	-0.073 12 / 2 / 20 0.979	-0.068 10 / 2 / 22 0.984	-0.061 14 / 2 / 18 0.929	-0.046 11 / 4 / 19 0.977	-0.034 13 / 4 / 17 0.842	-	0.052 19 / 1 / 14 0.112	<b>0.208</b> <b>27 / 3 / 4</b> <b>≤ 1e-03</b>
NCDE 0.456	-0.286 5 / 0 / 29 1.000	-0.244 3 / 0 / 31 1.000	-0.218 4 / 0 / 30 1.000	-0.188 7 / 0 / 27 1.000	-0.124 5 / 1 / 28 1.000	-0.120 10 / 2 / 22 0.998	-0.112 8 / 1 / 25 0.999	-0.098 10 / 2 / 22 0.996	-0.086 9 / 2 / 23 0.972	-0.052 14 / 1 / 19 0.886	-	<b>0.157</b> <b>25 / 1 / 8</b> <b>≤ 1e-03</b>
SVM 0.300	-0.442 3 / 2 / 29 1.000	-0.400 3 / 1 / 30 1.000	-0.375 3 / 1 / 30 1.000	-0.345 2 / 1 / 31 1.000	-0.281 5 / 2 / 27 1.000	-0.276 7 / 2 / 25 1.000	-0.269 4 / 2 / 28 1.000	-0.254 3 / 3 / 28 1.000	-0.242 3 / 5 / 26 1.000	-0.208 4 / 3 / 27 1.000	-0.157 8 / 1 / 25 1.000	If in bold, then p-value < 0.05

(b) Accuracy.

Figure 12: Summary performance statistics for the 12 classifiers on 34 datasets, generated using the multiple comparison matrix (MCM). The MCM shows pairwise comparisons. Each cell shows the mean difference in performance, wins/draws/losses, and Wilcoxon p-value for two comparates. The best models on the top left are sorted based on the average performance. The more intense the color, the higher the mean accuracy difference w.r.t. the compare, positive (red) or negative (blue).

	ROCKET 0.677	BORF 0.650	LGBM 0.619	RIFC 0.600	TIMESNET 0.550	SAITS 0.548	KNN 0.548	RAINDROP 0.543	BRITS 0.507	GRU-D 0.464	NCDE 0.415	SVM 0.269
Mean-precision	1	1	1	1	1	1	1	1	1	1	1	1
ROCKET 0.677	Mean-Difference -0.027 rsc / rsc / rsc Wilcoxon p-value <b>0.002</b>	<b>0.027</b> 24 / 3 / 7 <b>0.006</b>	<b>0.058</b> 24 / 3 / 7 <b>0.001</b>	<b>0.077</b> 26 / 4 / 4 <b>0.001</b>	<b>0.127</b> 24 / 0 / 10 <b>0.002</b>	<b>0.128</b> 26 / 0 / 8 <b>0.005</b>	<b>0.128</b> 27 / 1 / 6 <b>0.001</b>	<b>0.133</b> 26 / 0 / 8 <b>0.001</b>	<b>0.169</b> 25 / 0 / 9 <b>0.002</b>	<b>0.213</b> 24 / 1 / 9 <b>0.001</b>	<b>0.261</b> 26 / 0 / 8 <b>≤ 1e-03</b>	<b>0.408</b> 29 / 2 / 3 <b>≤ 1e-03</b>
BORF 0.650	-0.027 7 / 3 / 24 0.998	-	0.031 19 / 4 / 11 0.074	<b>0.050</b> 20 / 3 / 11 <b>0.024</b>	<b>0.099</b> 22 / 0 / 12 <b>0.016</b>	<b>0.101</b> 24 / 0 / 10 <b>0.014</b>	<b>0.101</b> 21 / 0 / 13 <b>0.047</b>	<b>0.106</b> 24 / 0 / 10 <b>0.005</b>	<b>0.142</b> 22 / 0 / 12 <b>0.008</b>	<b>0.186</b> 25 / 0 / 9 <b>0.001</b>	<b>0.234</b> 28 / 0 / 6 <b>≤ 1e-03</b>	<b>0.381</b> 29 / 1 / 4 <b>≤ 1e-03</b>
LGBM 0.619	-0.058 7 / 3 / 24 0.994	-0.031 11 / 4 / 19 0.926	-	0.019 19 / 3 / 12 0.104	<b>0.069</b> 21 / 0 / 13 <b>0.005</b>	<b>0.071</b> 23 / 0 / 11 <b>0.014</b>	0.071 21 / 0 / 13 0.081	<b>0.076</b> 23 / 0 / 11 <b>0.005</b>	<b>0.112</b> 24 / 0 / 10 <b>0.005</b>	<b>0.155</b> 26 / 0 / 8 <b>0.001</b>	<b>0.204</b> 29 / 0 / 5 <b>≤ 1e-03</b>	<b>0.350</b> 30 / 1 / 3 <b>≤ 1e-03</b>
RIFC 0.600	-0.077 4 / 4 / 26 0.999	-0.050 11 / 3 / 20 0.976	-0.019 12 / 3 / 19 0.896	-	0.050 19 / 0 / 15 0.107	<b>0.051</b> 22 / 0 / 12 <b>0.045</b>	0.051 21 / 0 / 13 0.176	<b>0.056</b> 23 / 0 / 11 <b>0.032</b>	<b>0.092</b> 22 / 0 / 12 <b>0.024</b>	<b>0.136</b> 25 / 0 / 9 <b>0.002</b>	<b>0.184</b> 27 / 0 / 7 <b>0.001</b>	<b>0.331</b> 29 / 1 / 4 <b>≤ 1e-03</b>
TIMESNET 0.550	-0.127 10 / 0 / 24 0.998	-0.099 12 / 0 / 22 0.985	-0.069 13 / 0 / 21 0.995	-0.050 15 / 0 / 19 0.896	-	0.002 19 / 2 / 13 0.316	0.002 14 / 2 / 18 0.684	0.007 13 / 2 / 19 0.095	0.043 19 / 3 / 12 0.095	<b>0.087</b> 22 / 2 / 10 <b>0.001</b>	<b>0.135</b> 23 / 1 / 10 <b>≤ 1e-03</b>	<b>0.281</b> 29 / 2 / 3 <b>≤ 1e-03</b>
SAITS 0.548	-0.128 8 / 0 / 26 0.995	-0.101 10 / 0 / 24 0.986	-0.071 11 / 0 / 23 0.987	-0.051 12 / 0 / 22 0.956	-0.002 13 / 2 / 19 0.684	-	0.000 12 / 2 / 20 0.748	0.005 13 / 2 / 19 0.608	0.041 16 / 2 / 16 0.201	<b>0.085</b> 19 / 2 / 13 <b>0.029</b>	<b>0.133</b> 28 / 1 / 5 <b>≤ 1e-03</b>	<b>0.279</b> 29 / 2 / 3 <b>≤ 1e-03</b>
KNN 0.548	-0.128 6 / 1 / 27 0.999	-0.101 13 / 0 / 21 0.955	-0.071 13 / 0 / 21 0.921	-0.051 13 / 0 / 21 0.829	-0.002 18 / 2 / 14 0.316	-0.000 20 / 2 / 12 0.252	-	0.005 16 / 3 / 15 0.236	0.041 16 / 3 / 15 0.278	<b>0.085</b> 20 / 4 / 10 <b>0.037</b>	<b>0.133</b> 23 / 2 / 9 <b>0.008</b>	<b>0.279</b> 26 / 5 / 3 <b>≤ 1e-03</b>
RAINDROP 0.543	-0.133 8 / 0 / 26 0.999	-0.106 10 / 0 / 24 0.995	-0.076 11 / 0 / 23 0.995	-0.056 11 / 0 / 23 0.969	-0.007 19 / 2 / 13 0.316	-0.005 19 / 2 / 13 0.392	-0.005 14 / 2 / 18 0.764	-	0.036 15 / 2 / 17 0.211	<b>0.080</b> 20 / 2 / 12 <b>0.018</b>	<b>0.128</b> 26 / 1 / 7 <b>≤ 1e-03</b>	<b>0.274</b> 28 / 3 / 3 <b>≤ 1e-03</b>
BRITS 0.507	-0.169 9 / 0 / 25 0.998	-0.142 12 / 0 / 22 0.992	-0.112 10 / 0 / 24 0.995	-0.092 12 / 0 / 22 0.977	-0.043 12 / 3 / 19 0.799	-0.041 16 / 2 / 16 0.722	-0.041 15 / 3 / 16 0.779	-0.036 17 / 2 / 15 0.789	-	0.044 20 / 4 / 10 0.059	<b>0.092</b> 23 / 1 / 10 <b>0.004</b>	<b>0.238</b> 29 / 3 / 6 <b>≤ 1e-03</b>
GRU-D 0.464	-0.213 9 / 1 / 24 0.999	-0.186 9 / 0 / 25 0.999	-0.155 8 / 0 / 26 0.999	-0.136 9 / 0 / 25 0.998	-0.087 10 / 2 / 22 0.985	-0.085 13 / 2 / 19 0.971	-0.085 10 / 4 / 20 0.963	-0.080 12 / 2 / 20 0.982	-0.044 10 / 4 / 20 0.941	-	0.048 17 / 1 / 16 0.137	<b>0.195</b> 24 / 3 / 7 <b>≤ 1e-03</b>
NCDE 0.415	-0.261 8 / 0 / 26 1.000	-0.234 6 / 0 / 28 1.000	-0.204 5 / 0 / 29 1.000	-0.184 7 / 0 / 27 0.999	-0.135 10 / 1 / 23 0.999	-0.133 9 / 1 / 28 1.000	-0.133 9 / 2 / 23 0.992	-0.128 10 / 1 / 23 1.000	0.092 10 / 1 / 23 0.996	-0.048 16 / 1 / 17 0.863	-	<b>0.146</b> 24 / 1 / 9 <b>0.001</b>
SVM 0.269	-0.408 3 / 2 / 29 1.000	-0.381 4 / 1 / 29 1.000	-0.350 3 / 1 / 30 1.000	-0.331 4 / 1 / 29 1.000	-0.281 3 / 2 / 29 1.000	-0.279 3 / 2 / 29 1.000	-0.279 3 / 5 / 26 1.000	-0.274 3 / 3 / 28 1.000	-0.238 6 / 3 / 25 1.000	-0.195 7 / 3 / 24 1.000	-0.146 9 / 1 / 24 0.999	<b>If in bold, then p-value &lt; 0.05</b>

(a) Precision.

	ROCKET 0.691	BORF 0.645	LGBM 0.625	RIFC 0.591	TIMESNET 0.540	RAINDROP 0.538	KNN 0.535	SAITS 0.533	BRITS 0.506	GRU-D 0.466	NCDE 0.423	SVM 0.283
Mean-recall	1	1	1	1	1	1	1	1	1	1	1	1
ROCKET 0.691	Mean-Difference -0.047 rsc / rsc / rsc Wilcoxon p-value <b>0.001</b>	<b>0.067</b> 22 / 4 / 8 <b>0.001</b>	<b>0.067</b> 24 / 4 / 6 <b>0.001</b>	<b>0.100</b> 26 / 4 / 4 <b>≤ 1e-03</b>	<b>0.151</b> 25 / 1 / 8 <b>≤ 1e-03</b>	<b>0.153</b> 27 / 1 / 6 <b>≤ 1e-03</b>	<b>0.156</b> 27 / 1 / 6 <b>≤ 1e-03</b>	<b>0.158</b> 26 / 0 / 8 <b>≤ 1e-03</b>	<b>0.186</b> 26 / 0 / 8 <b>≤ 1e-03</b>	<b>0.226</b> 24 / 1 / 9 <b>≤ 1e-03</b>	<b>0.268</b> 27 / 0 / 7 <b>≤ 1e-03</b>	<b>0.409</b> 30 / 2 / 2 <b>≤ 1e-03</b>
BORF 0.645	-0.047 8 / 4 / 26 0.999	-	0.020 19 / 4 / 11 0.074	<b>0.053</b> 22 / 4 / 8 <b>0.013</b>	<b>0.104</b> 22 / 1 / 11 <b>0.004</b>	<b>0.106</b> 24 / 3 / 9 <b>0.026</b>	<b>0.110</b> 20 / 0 / 14 <b>0.003</b>	<b>0.111</b> 24 / 0 / 10 <b>0.003</b>	<b>0.139</b> 22 / 0 / 12 <b>0.006</b>	<b>0.179</b> 23 / 0 / 11 <b>≤ 1e-03</b>	<b>0.221</b> 28 / 0 / 6 <b>≤ 1e-03</b>	<b>0.362</b> 30 / 1 / 3 <b>≤ 1e-03</b>
LGBM 0.625	-0.067 6 / 4 / 24 0.999	-0.020 11 / 4 / 19 0.926	-	0.033 19 / 4 / 11 0.072	<b>0.085</b> 21 / 1 / 12 <b>0.002</b>	<b>0.087</b> 23 / 0 / 10 <b>0.001</b>	0.090 19 / 1 / 14 0.071	<b>0.092</b> 22 / 0 / 12 <b>0.004</b>	<b>0.119</b> 24 / 0 / 10 <b>0.001</b>	<b>0.159</b> 24 / 0 / 10 <b>≤ 1e-03</b>	<b>0.202</b> 29 / 0 / 5 <b>≤ 1e-03</b>	<b>0.342</b> 30 / 1 / 3 <b>≤ 1e-03</b>
RIFC 0.591	-0.100 4 / 4 / 26 1.000	-0.053 8 / 4 / 22 0.987	-0.033 11 / 4 / 19 0.928	-	<b>0.051</b> 22 / 1 / 11 <b>0.044</b>	<b>0.053</b> 22 / 1 / 11 <b>0.026</b>	0.056 21 / 0 / 13 0.098	<b>0.058</b> 23 / 1 / 10 <b>0.020</b>	<b>0.086</b> 24 / 0 / 10 <b>0.012</b>	<b>0.125</b> 25 / 0 / 9 <b>0.001</b>	<b>0.168</b> 26 / 0 / 8 <b>≤ 1e-03</b>	<b>0.309</b> 31 / 1 / 2 <b>≤ 1e-03</b>
TIMESNET 0.540	-0.151 8 / 1 / 25 1.000	-0.104 11 / 1 / 22 0.996	-0.085 12 / 1 / 21 0.996	-0.051 11 / 1 / 22 0.956	-	0.002 15 / 3 / 16 0.585	0.005 14 / 2 / 18 0.678	0.034 19 / 2 / 13 0.252	0.034 21 / 3 / 10 0.065	<b>0.074</b> 22 / 2 / 10 <b>0.012</b>	<b>0.117</b> 23 / 1 / 10 <b>≤ 1e-03</b>	<b>0.257</b> 26 / 3 / 5 <b>≤ 1e-03</b>
RAINDROP 0.538	-0.153 6 / 1 / 27 1.000	-0.106 9 / 1 / 24 0.999	-0.087 10 / 1 / 23 0.999	-0.053 11 / 1 / 22 0.974	-0.002 16 / 3 / 15 0.415	-	0.003 16 / 2 / 16 0.640	0.005 21 / 2 / 11 0.231	0.032 19 / 2 / 13 0.148	<b>0.072</b> 20 / 2 / 12 <b>0.016</b>	<b>0.115</b> 26 / 1 / 7 <b>≤ 1e-03</b>	<b>0.255</b> 28 / 3 / 3 <b>≤ 1e-03</b>
KNN 0.535	-0.156 6 / 1 / 27 1.000	-0.110 14 / 0 / 20 0.975	-0.090 14 / 1 / 19 0.929	-0.056 13 / 0 / 21 0.905	-0.003 18 / 2 / 14 0.322	-0.003 16 / 2 / 16 0.360	-	0.002 19 / 2 / 13 0.356	0.029 15 / 4 / 15 0.095	0.069 17 / 4 / 13 0.011	<b>0.112</b> 23 / 2 / 9 <b>0.011</b>	<b>0.252</b> 26 / 6 / 2 <b>≤ 1e-03</b>
SAITS 0.533	-0.158 8 / 0 / 26 1.000	-0.111 10 / 0 / 24 0.997	-0.092 12 / 0 / 22 0.996	-0.058 10 / 1 / 23 0.980	-0.007 13 / 2 / 19 0.748	-0.005 11 / 2 / 21 0.769	-0.002 13 / 2 / 19 0.731	-	0.027 16 / 2 / 16 0.280	<b>0.067</b> 19 / 2 / 13 <b>0.039</b>	<b>0.110</b> 27 / 1 / 6 <b>≤ 1e-03</b>	<b>0.250</b> 29 / 2 / 3 <b>≤ 1e-03</b>
BRITS 0.506	-0.186 8 / 0 / 26 1.000	-0.139 12 / 0 / 22 0.999	-0.119 10 / 0 / 24 0.999	-0.086 10 / 0 / 24 0.988	-0.034 10 / 3 / 21 0.935	-0.032 13 / 2 / 19 0.852	-0.029 15 / 4 / 15 0.644	-0.027 16 / 2 / 16 0.720	-	0.040 17 / 4 / 13 0.082	<b>0.083</b> 23 / 1 / 10 <b>0.005</b>	<b>0.223</b> 27 / 3 / 4 <b>≤ 1e-03</b>
GRU-D 0.466	-0.226 9 / 1 / 24 1.000	-0.179 11 / 0 / 23 1.000	-0.159 10 / 0 / 24 1.000	-0.125 9 / 0 / 25 0.999	-0.074 10 / 2 / 22 0.988	-0.072 12 / 2 / 20 0.905	-0.069 13 / 4 / 17 0.961	-0.067 13 / 2 / 19 0.918	-0.040 13 / 4 / 17 0.918	-	0.043 18 / 1 / 15 0.137	<b>0.183</b> 27 / 3 / 4 <b>≤ 1e-03</b>
NCDE 0.423	-0.268 7 / 0 / 27 1.000	-0.221 6 / 0 / 28 1.000	-0.202 5 / 0 / 29 1.000	-0.168 8 / 0 / 26 0.999	-0.117 10 / 1 / 23 0.999	-0.115 7 / 1 / 26 1.000	-0.112 9 / 2 / 23 0.989	-0.110 6 / 1 / 27 1.000	-0.083 10 / 1 / 23 0.995	-0.043 15 / 1 / 18 0.863	-	<b>0.140</b> 27 / 1 / 6 <b>≤ 1e-03</b>
SVM 0.283	-0.409 2 / 2 / 30 1.000	-0.362 3 / 1 / 30 1.000	-0.342 3 / 1 / 30 1.000	-0.309 2 / 1 / 31 1.000	-0.257 5 / 3 / 26 1.000	-0.255 3 / 3 / 28 1.000	-0.252 2 / 6 / 26 1.000	-0.250 3 / 2 / 29 1.000	-0.223 4 / 3 / 27 1.000	-0.183 6 / 1 / 27 1.000	-0.140 6 / 1 / 27 1.000	<b>If in bold, then p-value &lt; 0.05</b>

(b) Recall.

Figure 13: Summary performance statistics for the 12 classifiers on 34 datasets, generated using the multiple comparison matrix (MCM). The MCM shows pairwise comparisons. Each cell shows the mean difference in performance, wins/draws/losses, and Wilcoxon p-value for two comparates. The best models on the top left are sorted based on the average performance. The more intense the color, the higher the mean accuracy difference w.r.t. the compare, positive (red) or negative (blue).

	LGBM 472.791	ROCKET 1485.083	RIFC 1656.918	BORF 5298.659	NCDE 6877.340	GRU-D 9351.653	TIMESNET 12925.685	KNN 16523.164	RAINDROP 18921.227	SVM 21772.918	SAITS 30426.722	BRITS 60025.019
Mean-total time	1	1	1	1	1	1	1	1	1	1	1	1
LGBM	Mean-Difference rsc / rsc / rsc Wilcoxon p-value	-1012.291 22 / 0 / 12 ≤ 1e-03	-1184.127 14 / 0 / 20 0.058	-4825.868 5 / 0 / 29 1.000	-6404.549 13 / 0 / 21 0.902	-8878.861 3 / 0 / 31 1.000	-12452.894 0 / 0 / 34 1.000	-16050.373 8 / 0 / 26 0.999	-18448.436 12 / 0 / 22 1.000	-21300.127 10 / 0 / 24 1.000	-29953.930 0 / 0 / 34 1.000	-59552.228 0 / 0 / 34 1.000
ROCKET	1012.291 5 / 0 / 29 1.000	1	-171.836 18 / 0 / 16 0.407	-3813.576 5 / 0 / 29 1.000	-5392.258 1 / 0 / 33 1.000	-7866.570 1 / 0 / 33 1.000	-11440.602 0 / 0 / 34 1.000	-15038.081 1 / 0 / 33 1.000	-17436.145 0 / 0 / 34 1.000	-20287.836 0 / 0 / 34 1.000	-28941.639 0 / 0 / 34 1.000	-58539.936 0 / 0 / 34 1.000
1485.083	1184.127 12 / 0 / 22 0.944	171.836 16 / 0 / 18 0.600	1	-3641.741 2 / 0 / 32 1.000	-5220.422 2 / 0 / 32 1.000	-7694.734 1 / 0 / 33 1.000	-11268.767 1 / 0 / 33 1.000	-14866.246 2 / 0 / 32 1.000	-17264.309 1 / 0 / 33 1.000	-20116.000 1 / 0 / 33 1.000	-28769.803 1 / 0 / 33 1.000	-58368.101 1 / 0 / 33 1.000
RIFC	4825.868 20 / 0 / 14 0.159	3813.576 29 / 0 / 5 ≤ 1e-03	3641.741 32 / 0 / 2 ≤ 1e-03	1	-1578.682 13 / 0 / 21 0.837	-4052.984 3 / 0 / 31 1.000	-7627.026 2 / 0 / 32 1.000	-11224.505 8 / 0 / 26 1.000	-13622.568 5 / 0 / 29 1.000	-16474.260 7 / 0 / 27 1.000	-25126.063 2 / 0 / 32 1.000	-54726.360 1 / 0 / 33 1.000
5298.659	6404.549 21 / 0 / 13 0.101	5392.258 33 / 0 / 1 ≤ 1e-03	5220.422 32 / 0 / 2 ≤ 1e-03	1578.682 21 / 0 / 13 0.167	1	-2474.312 10 / 1 / 23 0.998	-6048.345 5 / 1 / 28 0.993	-9645.823 15 / 1 / 17 0.993	-12043.887 14 / 1 / 19 1.000	-14895.578 14 / 1 / 19 1.000	-23549.381 4 / 1 / 29 1.000	-53147.678 2 / 1 / 31 1.000
6877.340	8878.861 31 / 0 / 3 ≤ 1e-03	7866.570 33 / 0 / 1 ≤ 1e-03	7694.734 31 / 0 / 3 ≤ 1e-03	4052.994 31 / 0 / 3 ≤ 1e-03	2474.312 23 / 1 / 10 0.002	1	-3574.032 4 / 2 / 28 1.000	-7171.511 19 / 2 / 13 0.672	-9569.575 21 / 2 / 11 0.335	-12421.266 23 / 2 / 9 0.196	-21075.069 1 / 2 / 31 1.000	-50673.266 0 / 2 / 32 1.000
GRU-D	12452.894 28 / 2 / 5 ≤ 1e-03	11440.602 33 / 0 / 1 ≤ 1e-03	11268.767 32 / 0 / 2 ≤ 1e-03	7627.026 28 / 2 / 5 ≤ 1e-03	6048.345 16 / 1 / 21 0.002	3574.032 31 / 0 / 31 ≤ 1e-03	1	-3597.479 24 / 2 / 8 0.097	-5995.542 27 / 2 / 5 0.001	-8847.233 27 / 2 / 5 0.002	-17501.037 4 / 2 / 28 1.000	-47099.334 2 / 2 / 30 1.000
9351.653	16050.373 26 / 0 / 8 ≤ 1e-03	15038.081 33 / 0 / 1 ≤ 1e-03	14866.246 32 / 0 / 2 ≤ 1e-03	11224.505 26 / 0 / 8 ≤ 1e-03	9645.823 17 / 2 / 15 0.016	7171.511 13 / 2 / 19 0.328	3597.479 8 / 2 / 24 0.903	1	-2398.063 16 / 2 / 16 0.221	-5249.755 13 / 3 / 18 0.551	-13903.558 3 / 2 / 29 1.000	-43501.855 1 / 2 / 31 1.000
16523.164	18448.436 22 / 0 / 12 0.012	17436.145 33 / 0 / 1 ≤ 1e-03	17264.309 32 / 0 / 2 ≤ 1e-03	13622.568 29 / 0 / 5 ≤ 1e-03	12043.887 16 / 1 / 21 0.178	9569.575 5 / 2 / 27 0.665	5995.542 16 / 2 / 16 0.779	2398.063 18 / 2 / 16 0.999	1	-2851.691 16 / 2 / 16 0.684	-11505.494 2 / 2 / 30 1.000	-41103.792 1 / 2 / 31 1.000
RAINDROP	21300.127 24 / 0 / 10 0.001	20287.836 33 / 0 / 1 ≤ 1e-03	20116.000 32 / 0 / 2 ≤ 1e-03	16474.260 27 / 0 / 7 ≤ 1e-03	14895.578 19 / 1 / 14 0.004	12421.266 9 / 2 / 23 0.804	8847.233 5 / 2 / 27 0.007	5249.755 18 / 3 / 13 0.316	2851.691 16 / 2 / 16 1.000	1	-8653.803 3 / 2 / 29 1.000	-38252.100 1 / 2 / 31 1.000
21772.918	29953.930 34 / 0 / 0 ≤ 1e-03	28941.639 33 / 0 / 1 ≤ 1e-03	28769.803 32 / 0 / 2 ≤ 1e-03	25126.063 29 / 1 / 4 ≤ 1e-03	23549.381 31 / 2 / 1 ≤ 1e-03	21075.069 28 / 2 / 4 ≤ 1e-03	17501.037 29 / 2 / 3 ≤ 1e-03	13903.558 29 / 2 / 3 ≤ 1e-03	11505.494 30 / 2 / 2 ≤ 1e-03	8653.803 29 / 2 / 3 ≤ 1e-03	1	-39598.297 4 / 2 / 28 1.000
SAITS	59552.228 34 / 0 / 0 ≤ 1e-03	58539.936 33 / 0 / 1 ≤ 1e-03	58368.101 32 / 0 / 2 ≤ 1e-03	54726.360 33 / 0 / 1 ≤ 1e-03	53147.678 31 / 2 / 3 ≤ 1e-03	50673.266 32 / 2 / 0 ≤ 1e-03	47099.334 30 / 2 / 2 ≤ 1e-03	43501.855 31 / 2 / 1 ≤ 1e-03	41103.792 31 / 2 / 1 ≤ 1e-03	38252.100 31 / 2 / 1 ≤ 1e-03	29598.297 28 / 2 / 4 ≤ 1e-03	If in bold, then p-value < 0.05
60025.019												

(a) Total Runtime.

	ROCKET 0.851	BORF 0.844	LGBM 0.832	RIFC 0.815	SAITS 0.748	RAINDROP 0.744	TIMESNET 0.741	BRITS 0.736	GRU-D 0.718	KNN 0.701	NCDE 0.693	SVM 0.493
Mean-roc_auc	1	1	1	1	1	1	1	1	1	1	1	1
ROCKET	Mean-Difference rsc / rsc / rsc Wilcoxon p-value	0.007 23 / 4 / 7 0.007	0.019 21 / 4 / 9 0.021	0.036 27 / 4 / 3 ≤ 1e-03	0.104 27 / 0 / 7 0.002	0.108 27 / 1 / 6 0.001	0.111 27 / 0 / 7 ≤ 1e-03	0.115 25 / 1 / 8 0.002	0.133 25 / 0 / 9 ≤ 1e-03	0.151 30 / 0 / 4 ≤ 1e-03	0.158 27 / 0 / 7 ≤ 1e-03	0.358 31 / 1 / 2 ≤ 1e-03
0.851	-0.007 7 / 4 / 23 0.993	1	0.012 18 / 4 / 12 0.128	0.029 22 / 4 / 8 0.007	0.097 27 / 0 / 7 0.001	0.101 25 / 1 / 8 0.001	0.108 24 / 0 / 10 ≤ 1e-03	0.126 22 / 1 / 11 0.004	0.144 22 / 0 / 12 0.001	0.151 23 / 0 / 11 0.005	0.151 29 / 0 / 5 ≤ 1e-03	0.351 30 / 1 / 3 ≤ 1e-03
BORF	-0.019 9 / 4 / 21 0.979	-0.012 12 / 4 / 18 0.872	1	0.017 20 / 4 / 10 0.057	0.085 24 / 0 / 10 ≤ 1e-03	0.089 27 / 1 / 6 ≤ 1e-03	0.092 25 / 0 / 9 ≤ 1e-03	0.096 23 / 1 / 10 0.001	0.114 26 / 0 / 8 0.002	0.132 21 / 0 / 13 ≤ 1e-03	0.139 29 / 0 / 5 ≤ 1e-03	0.339 30 / 1 / 3 ≤ 1e-03
LGBM	-0.036 3 / 4 / 27 1.000	-0.029 8 / 4 / 22 0.993	-0.017 10 / 4 / 20 0.943	1	0.068 24 / 0 / 10 0.026	0.072 21 / 1 / 12 0.045	0.075 21 / 0 / 13 0.030	0.080 21 / 1 / 12 0.016	0.098 24 / 0 / 10 0.003	0.115 22 / 0 / 12 0.023	0.122 26 / 0 / 8 0.002	0.322 31 / 1 / 2 ≤ 1e-03
0.832	-0.104 7 / 0 / 27 0.988	-0.097 7 / 0 / 27 0.999	-0.085 10 / 0 / 24 0.996	-0.068 10 / 0 / 24 0.975	1	0.004 14 / 2 / 18 0.678	0.007 13 / 2 / 19 0.702	0.012 14 / 12 / 18 0.425	0.030 20 / 2 / 12 0.091	0.047 13 / 2 / 19 0.541	0.054 25 / 1 / 8 0.010	0.254 29 / 2 / 3 ≤ 1e-03
0.844	-0.108 6 / 1 / 27 0.999	-0.101 8 / 1 / 25 0.999	-0.089 6 / 1 / 27 1.000	-0.072 12 / 1 / 21 0.955	-0.004 18 / 2 / 14 0.322	0.003 17 / 2 / 15 0.231	0.008 16 / 3 / 15 0.307	0.026 19 / 2 / 13 0.088	0.043 13 / 2 / 19 0.527	0.050 23 / 1 / 10 0.010	0.250 27 / 4 / 3 ≤ 1e-03	0.351 30 / 1 / 3 ≤ 1e-03
RAINDROP	-0.111 7 / 0 / 27 1.000	-0.104 10 / 0 / 24 1.000	-0.092 9 / 0 / 25 1.000	-0.075 13 / 0 / 21 0.971	-0.007 19 / 2 / 13 0.298	-0.003 15 / 2 / 17 0.769	1	0.005 18 / 2 / 14 0.298	0.023 21 / 2 / 11 0.058	0.040 13 / 2 / 19 0.601	0.047 23 / 1 / 10 0.052	0.247 26 / 2 / 6 ≤ 1e-03
0.741	-0.115 8 / 1 / 25 0.998	-0.108 11 / 1 / 22 0.996	-0.096 10 / 1 / 23 0.984	-0.080 12 / 1 / 21 0.975	-0.012 18 / 2 / 14 0.575	-0.008 15 / 3 / 16 0.693	-0.005 14 / 2 / 18 0.702	1	0.018 20 / 2 / 12 0.122	0.035 15 / 2 / 17 0.527	0.043 23 / 1 / 10 0.014	0.243 29 / 3 / 2 ≤ 1e-03
BRITS	-0.133 9 / 0 / 25 0.998	-0.126 12 / 0 / 22 0.999	-0.114 8 / 0 / 26 0.999	-0.098 10 / 0 / 24 0.997	-0.030 12 / 2 / 20 0.909	-0.026 13 / 2 / 19 0.912	-0.023 11 / 2 / 21 0.942	-0.018 12 / 2 / 20 0.878	1	-0.017 15 / 2 / 17 0.708	0.025 20 / 1 / 13 0.161	0.225 29 / 2 / 3 ≤ 1e-03
0.718	-0.151 4 / 0 / 30 1.000	-0.144 11 / 0 / 23 0.995	-0.132 13 / 0 / 21 0.976	-0.115 12 / 0 / 22 0.978	-0.047 19 / 2 / 13 0.459	-0.043 19 / 2 / 13 0.473	-0.040 19 / 2 / 13 0.399	-0.035 17 / 2 / 15 0.292	-0.017 17 / 2 / 15 0.292	1	0.007 20 / 2 / 12 0.152	0.207 26 / 6 / 2 ≤ 1e-03
KNN	-0.158 7 / 0 / 27 1.000	-0.151 5 / 0 / 29 1.000	-0.139 5 / 0 / 29 1.000	-0.122 8 / 0 / 26 0.998	-0.054 8 / 1 / 25 0.990	-0.050 10 / 1 / 23 0.948	-0.047 10 / 1 / 23 0.986	-0.043 10 / 1 / 23 0.839	0.025 13 / 1 / 20 0.848	-0.007 12 / 2 / 20 1.000	1	0.200 29 / 1 / 4 ≤ 1e-03
NCDE	-0.358 2 / 1 / 31 1.000	-0.351 3 / 1 / 30 1.000	-0.339 3 / 1 / 30 1.000	-0.322 2 / 1 / 31 1.000	-0.254 3 / 2 / 29 1.000	-0.250 3 / 4 / 27 1.000	-0.247 6 / 2 / 26 1.000	-0.243 2 / 3 / 29 1.000	-0.225 3 / 2 / 29 1.000	-0.207 2 / 6 / 26 1.000	-0.200 4 / 1 / 29 1.000	If in bold, then p-value < 0.05
0.493												

(b) ROC-AUC.

Figure 14: Summary performance statistics for the 12 classifiers on 34 datasets, generated using the multiple comparison matrix (MCM). The MCM shows pairwise comparisons. Each cell shows the mean difference in performance, wins/draws/losses, and Wilcoxon p-value for two comparates. The best models on the top left are sorted based on the average performance. The more intense the color, the higher the mean accuracy difference w.r.t. the comparate, positive (red) or negative (blue).

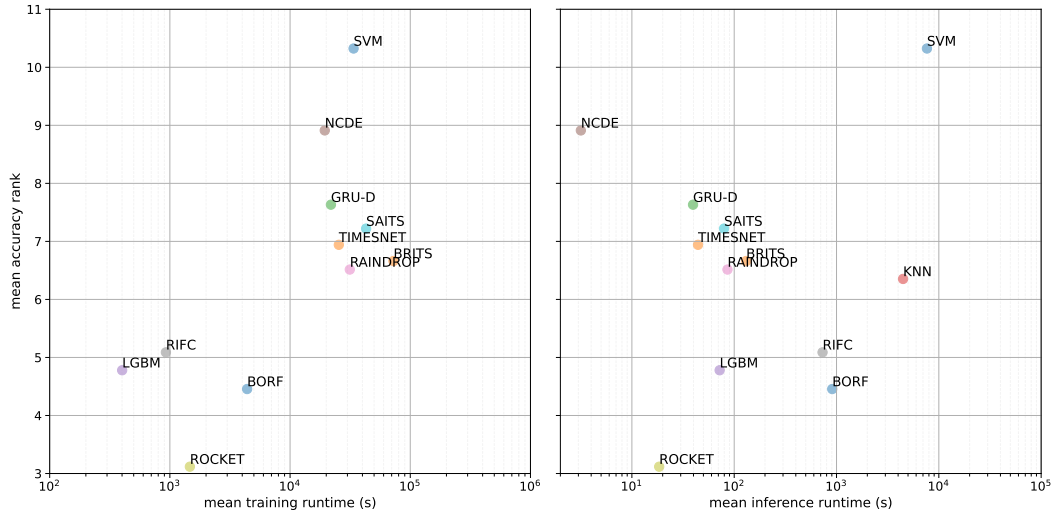


Table 6: F1 score on the test set for each dataset and each classifier. The average of 3 runs is taken for methods that highly depend upon initialization, i.e., all approaches besides BORF, KNN, LGBM, and SVM. Missing values are due to exceeding memory or maximum runtime. The best values for each dataset are in bold.

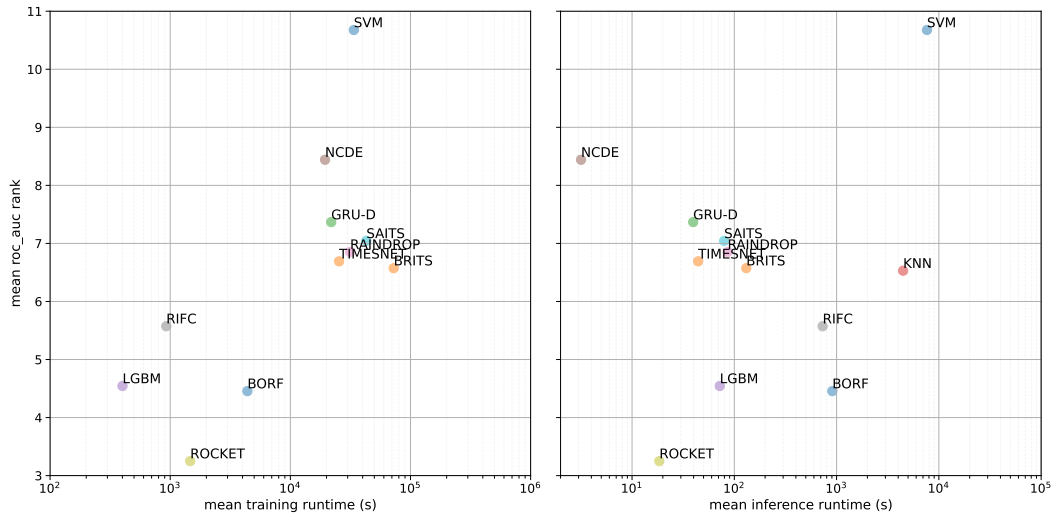
	BORF	BRITS	GRU-D	KNN	LGBM	NCDE	RAINDROP	RIFC	ROCKET	SAITS	SVM	TIMESNET
ABF	0.17	0.33±0.01	0.28±0.09	0.31	0.17	<b>0.41</b> ±0.02	0.27±0.01	0.17±0.00	0.17±0.00	0.30±0.03	0.32	0.31±0.01
AN	0.80	0.65±0.00	0.68±0.03	0.80	0.80	0.43±0.11	0.64±0.05	0.88±0.02	<b>0.90</b> ±0.04	0.59±0.03	0.07	0.61±0.01
AOC	<b>0.82</b>	0.30±0.00	0.31±0.28	0.64	0.68	0.51±0.01	0.66±0.03	0.68±0.03	0.80±0.01	0.75±0.02	0.02	0.62±0.03
APT	0.91	0.78±0.02	0.49±0.31	0.34	0.80	0.69±0.00	0.77±0.01	0.88±0.03	<b>0.96</b> ±0.00	0.84±0.01	0.05	0.86±0.02
ARC	0.95	0.99±0.00	0.63±0.10	0.36	0.95	0.81±0.00	0.97±0.01	0.77±0.28	<b>0.99</b> ±0.01	0.99±0.00	0.10	0.99±0.00
CT	0.94	0.96±0.05	0.64±0.30	<b>0.98</b>	0.95	0.87±0.01	0.97±0.00	0.94±0.02	0.98±0.00	0.94±0.05	0.68	0.95±0.02
DD	0.51	0.52±0.02	0.46±0.07	0.44	0.52	0.29±0.12	0.45±0.04	0.49±0.04	<b>0.54</b> ±0.03	0.43±0.06	0.23	0.20±0.02
DG	0.34	0.72±0.07	0.71±0.07	<b>0.90</b>	0.34	0.51±0.04	0.60±0.22	0.34±0.00	0.34±0.00	0.57±0.10	0.85	0.42±0.03
DW	0.42	0.93±0.02	0.63±0.27	<b>0.97</b>	0.42	0.80±0.13	0.78±0.31	0.42±0.00	0.42±0.00	0.96±0.01	0.96	0.63±0.02
GM1	0.58	0.47±0.04	0.24±0.08	0.33	0.57	0.23±0.02	0.46±0.11	0.49±0.02	<b>0.66</b> ±0.02	0.41±0.02	0.04	0.50±0.04
GM2	0.50	0.32±0.05	0.40±0.08	0.26	0.39	0.20±0.08	0.30±0.15	0.36±0.03	<b>0.57</b> ±0.05	0.24±0.25	0.13	0.45±0.03
GM3	0.34	0.22±0.02	0.06±0.02	0.14	0.25	0.17±0.01	0.31±0.03	0.26±0.05	<b>0.48</b> ±0.03	0.27±0.11	0.01	0.32±0.03
GP1	0.88	0.27±0.06	0.23±0.14	0.75	0.78	0.32±0.02	0.81±0.05	0.80±0.04	<b>0.89</b> ±0.02	0.75±0.02	0.16	0.73±0.06
GP2	0.79	0.31±0.04	0.56±0.24	0.74	0.73	0.35±0.01	0.63±0.10	0.76±0.05	<b>0.85</b> ±0.05	0.54±0.10	0.43	0.58±0.04
GS	0.41	-	-	-	0.13	<b>0.52</b> ±0.29	-	0.07±0.02	0.31±0.15	-	-	-
GX	0.55	0.09±0.09	0.11±0.04	0.65	0.50	0.13±0.05	0.44±0.08	0.47±0.11	<b>0.70</b> ±0.01	0.33±0.09	0.11	0.44±0.00
GY	0.64	0.18±0.07	0.13±0.07	0.65	0.55	0.26±0.01	0.46±0.04	0.49±0.14	<b>0.70</b> ±0.02	0.43±0.10	0.13	0.44±0.02
GZ	0.58	0.17±0.09	0.10±0.04	0.62	0.48	0.11±0.04	0.33±0.04	0.44±0.13	<b>0.69</b> ±0.01	0.19±0.12	0.06	0.33±0.02
IW	0.48	0.65±0.01	0.61±0.00	-	<b>0.71</b>	0.10±0.02	0.02±0.00	0.39±0.34	0.53±0.00	0.13±0.07	0.02	0.60±0.00
JV	0.71	0.96±0.00	0.96±0.01	0.96	0.93	0.57±0.02	0.94±0.02	0.89±0.10	0.94±0.01	0.96±0.01	0.47	<b>0.97</b> ±0.01
LPA	<b>0.73</b>	0.28±0.20	0.21±0.14	0.02	0.53	0.44±0.03	0.33±0.09	0.32±0.20	0.02±0.01	0.26±0.06	0.02	0.27±0.03
MI3	0.27	0.42±0.11	0.35±0.00	0.35	0.41	0.34±0.17	0.36±0.15	<b>0.56</b> ±0.22	0.35±0.00	0.46±0.10	0.35	0.42±0.11
MP	0.85	0.92±0.00	0.92±0.01	0.88	<b>0.96</b>	0.63±0.02	0.74±0.04	0.90±0.04	0.94±0.00	0.67±0.34	0.44	0.93±0.01
P12	0.51	0.46±0.00	0.61±0.02	0.12	0.55	0.49±0.01	0.56±0.02	<b>0.63</b> ±0.01	0.47±0.01	0.55±0.01	0.46	0.56±0.01
P19	0.71	0.49±0.00	0.55±0.02	-	<b>0.75</b>	-	0.69±0.01	0.66±0.03	0.71±0.01	0.72±0.00	0.05	0.71±0.01
PAM	0.53	-	-	-	0.33	-	-	0.37±0.32	<b>0.66</b> ±0.10	-	-	-
PGE	0.40	<b>0.78</b> ±0.00	<b>0.78</b> ±0.00	<b>0.78</b>	0.40	0.57±0.29	0.48±0.26	0.40±0.00	0.40±0.00	0.65±0.22	0.40	0.43±0.05
PGZ	0.46	0.34±0.03	0.26±0.14	0.61	0.54	0.30±0.02	0.46±0.34	0.60±0.12	<b>0.73</b> ±0.00	0.65±0.07	0.16	0.57±0.06
PL	<b>0.87</b>	0.36±0.04	0.20±0.10	0.64	0.71	0.28±0.01	0.53±0.03	0.47±0.02	0.85±0.01	0.39±0.06	0.20	0.45±0.02
SAD	0.98	0.99±0.00	0.99±0.00	0.97	0.97	0.74±0.01	0.98±0.00	0.65±0.42	0.98±0.00	0.95±0.01	0.62	<b>0.99</b> ±0.00
SE	0.47	0.48±0.15	0.49±0.17	0.38	0.42	0.33±0.08	0.40±0.15	<b>0.82</b> ±0.04	0.80±0.08	0.27±0.02	0.26	0.24±0.06
SGZ	0.75	0.34±0.05	0.38±0.08	0.77	0.65	0.12±0.05	0.46±0.04	0.75±0.08	<b>0.88</b> ±0.02	0.57±0.11	0.13	0.49±0.09
TA	0.42	0.23±0.00	0.23±0.00	-	<b>0.77</b>	0.33±0.01	0.25±0.02	0.38±0.06	0.57±0.01	0.25±0.01	-	0.25±0.01
VE	<b>0.97</b>	0.50±0.08	0.60±0.01	0.88	0.94	0.63±0.08	0.65±0.02	0.90±0.02	0.94±0.02	0.62±0.03	0.40	0.59±0.01

Table 7: Total runtime (seconds) for each dataset and each classifier. The average of 3 runs is taken for methods that highly depend upon initialization, i.e., all approaches besides BORF, KNN, LGBM, and SVM. Missing values are due to exceeding memory or maximum runtime. The best values for each dataset are in bold.

	BORF	BRITS	GRU-D	KNN	LGBM	NCDE	RAINDROP	RIFC	ROCKET	SAITS	SVM	TIMESNET
ABF	16	230±8	33±6	10	2	1290±2051	16±2	5±0	<b>1</b> ±0	76±16	20	65±12
AN	18	5952±510	121±24	8	12	93±24	23±4	2±0	<b>1</b> ±0	344±40	11	203±29
AOC	295	5572±906	1274±503	1318	139	92±28	94±2	<b>21</b> ±1	23±1	5764±903	1196	2601±438
APT	1000	47501±10144	9416±3823	32482	302	180±5	13014±21270	78±6	<b>38</b> ±0	113432±7034	14178	21283±1363
ARC	679	246725±140403	16236±5490	26775	144	175±60	88376±7613	68±5	<b>52</b> ±1	248253±10872	8021	18775±1290
CT	300	18061±4779	1542±719	2563	613	243±85	472±84	<b>72</b> ±4	191±3	3516±590	2898	1989±292
DD	20	1989±478	90±24	4	32	111±29	39±9	<b>2</b> ±0	7±0	404±84	22	232±30
DG	12	1063±215	41±6	3	1	111±68	19±9	1±0	<b>0</b> ±0	174±7	7	64±12
DW	12	1526±904	67±39	3	1	243±141	40±37	1±0	<b>0</b> ±0	223±103	7	310±378
GM1	18	10400±2849	477±163	95	346	158±42	76±19	<b>4</b> ±0	25±1	1156±169	102	586±104
GM2	20	15746±1939	466±86	94	364	188±100	156±37	<b>4</b> ±0	26±1	1528±459	103	1078±266
GM3	22	7442±1118	467±222	93	440	136±39	80±18	<b>4</b> ±0	28±1	1228±122	103	634±26
GP1	25	6802±5500	338±14	82	61	91±27	56±9	<b>3</b> ±0	5±0	1450±360	97	575±165
GP2	27	6579±1563	998±53	79	71	90±25	50±9	<b>3</b> ±0	5±0	1253±78	105	797±149
GS	5718	-	-	-	<b>1358</b>	4815±6530	-	1826±22	26010±136	-	-	-
GX	62	4846±1652	430±133	942	373	52±25	85±5	<b>7</b> ±0	17±1	2015±341	307	1202±373
GY	54	5314±447	612±77	939	374	59±11	78±2	<b>7</b> ±0	17±0	2519±362	311	1151±198
GZ	63	6439±3059	533±67	879	230	87±24	97±3	<b>7</b> ±0	17±1	2864±647	306	1194±225
IW	31587	7067±138	1460±62	-	4533	38767±8867	5937±1596	39775±851	<b>118</b> ±2	5257±248	279477	5825±1060
JV	23	289±79	51±0	48	133	92±27	89±7	35±2	<b>6</b> ±0	197±112	41	337±42
LPA	411	31534±11204	3854±303	447	278	186±10	10318±17149	46±1	<b>27</b> ±0	39939±5076	99	35634±26815
MT3	12	1421±335	41±10	3	3	76±16	14±2	6±0	<b>0</b> ±0	113±35	4	81±12
MP	26	6230±7	122±13	816	306	205±85	550±207	<b>18</b> ±1	142±1	1171±241	950	489±90
P12	5455	72508±32359	4182±948	40226	239	1204±205	7582±12025	1907±34	<b>22</b> ±1	9444±1250	5764	7817±1145
P19	30858	244447±112157	45315±6110	-	751	-	294468±72194	9243±919	<b>206</b> ±2	116971±22038	144163	51343±6196
PA2	77647	-	-	-	4004	-	-	<b>1179</b> ±97	22963±92	-	-	-
PGE	6	784±165	50±69	2	1	197±123	9±1	2±0	<b>0</b> ±0	39±25	2	21±3
PGZ	8	2182±670	245±142	11	<b>1</b>	110±28	30±15	1±0	1±0	365±63	8	197±15
PL	108	56920±23275	4615±3922	4017	452	106±2	5162±8392	<b>11</b> ±0	40±1	26156±2239	2666	7031±1167
SAD	8487	33021±5648	1829±133	17309	<b>82</b>	930±143	1966±398	675±53	103±1	6956±536	17106	6991±936
SE	204	80101±34115	1893±120	164	17	123±31	20918±2925	<b>9</b> ±0	39±1	59800±14909	2019	3122±594
SGZ	9	1821±119	267±29	12	28	115±69	25±5	<b>1</b> ±0	2±0	325±20	10	239±34
TA	16825	861475±86400	46781±20524	-	352	10592±6509	20576±7435	1305±19	<b>350</b> ±9	197788±30354	-	92470±29583
VE	127	76064±5836	1311±589	362	32	115±49	108±27	8±0	<b>6</b> ±0	10987±6396	976	2339±196

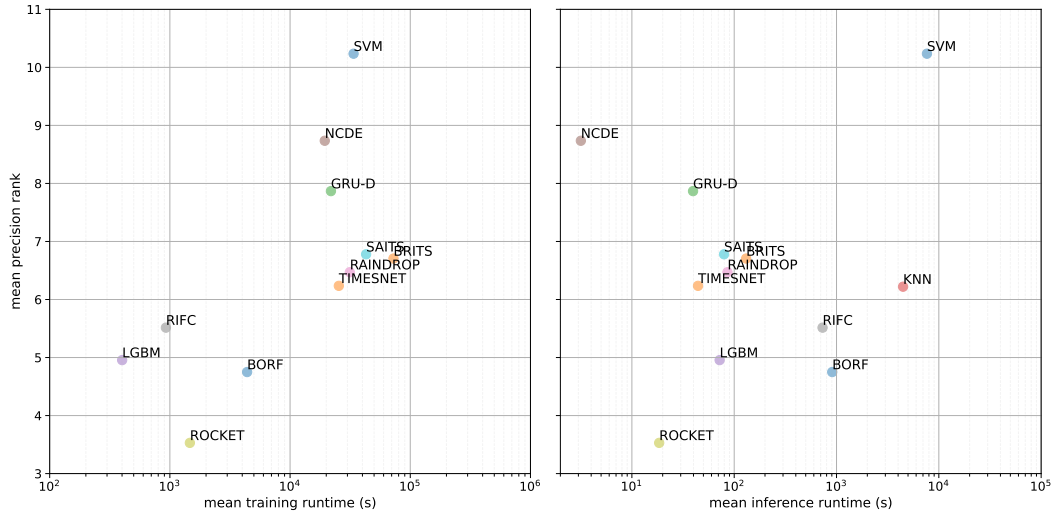


(a) Accuracy.

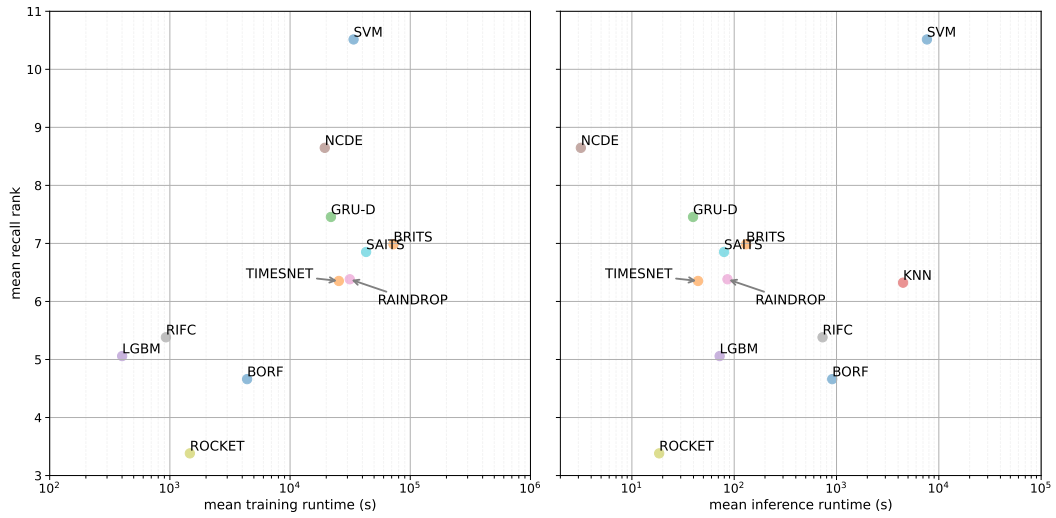


(b) ROC-AUC.

Figure 15: Average performance rank (lower is better) vs. training and inference runtimes (lower is better). Best values are on the bottom-left of each plot.

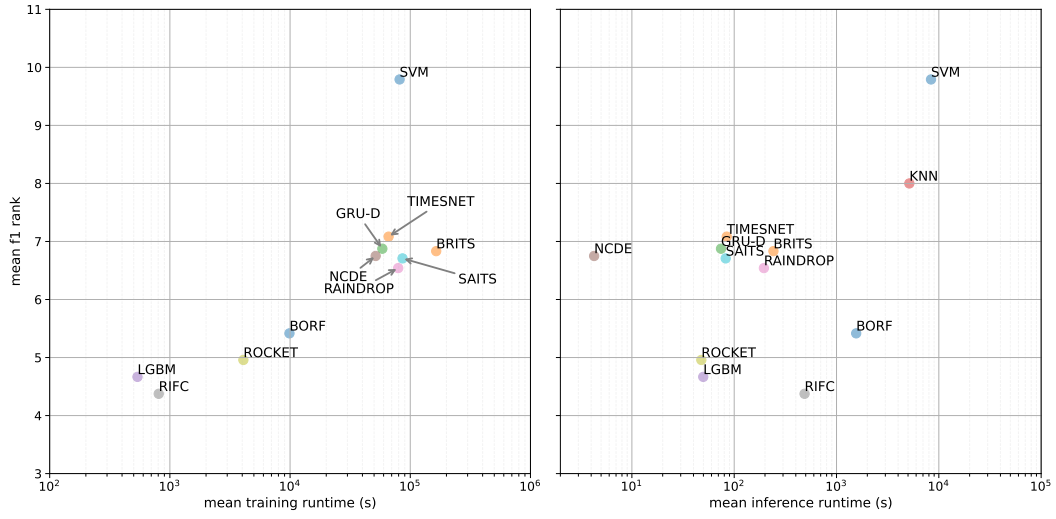


(a) Precision.

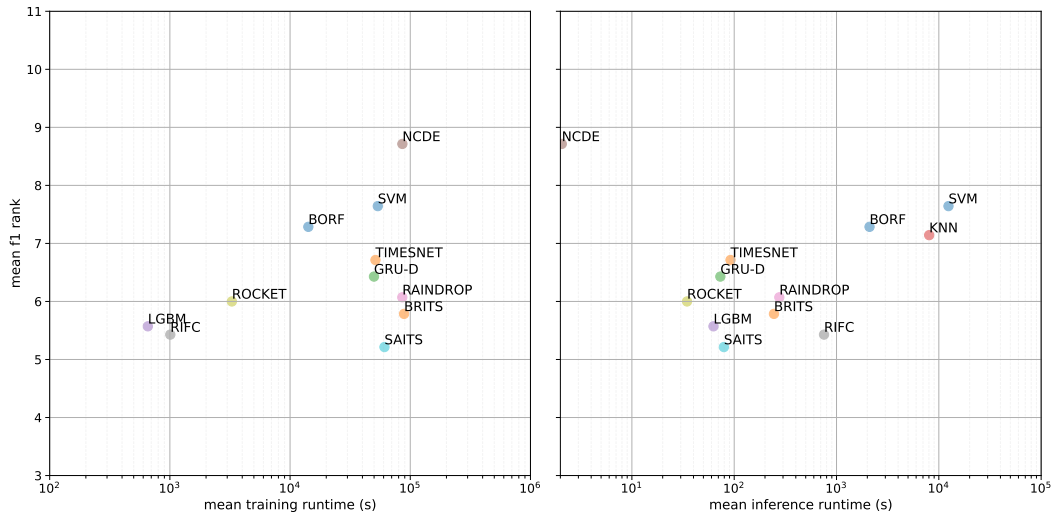


(b) Recall.

Figure 16: Average performance rank (lower is better) vs. training and inference runtimes (lower is better). Best values are on the bottom-left of each plot.

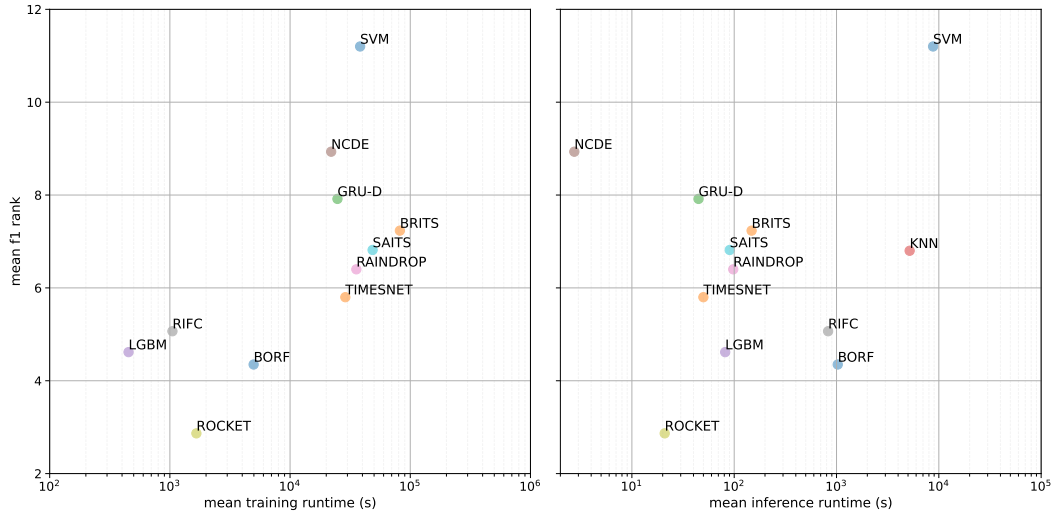


(a) Unevenly Sampled.

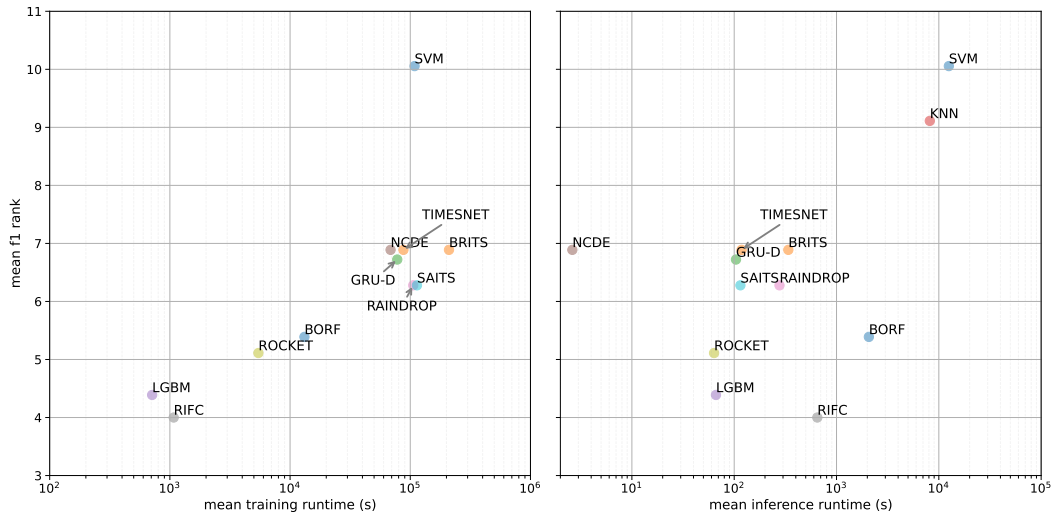


(b) Partially Observed.

Figure 17: Average F1 rank (lower is better) vs. training and inference runtimes (lower is better) for subsets of datasets. Best values are on the bottom-left of each plot.



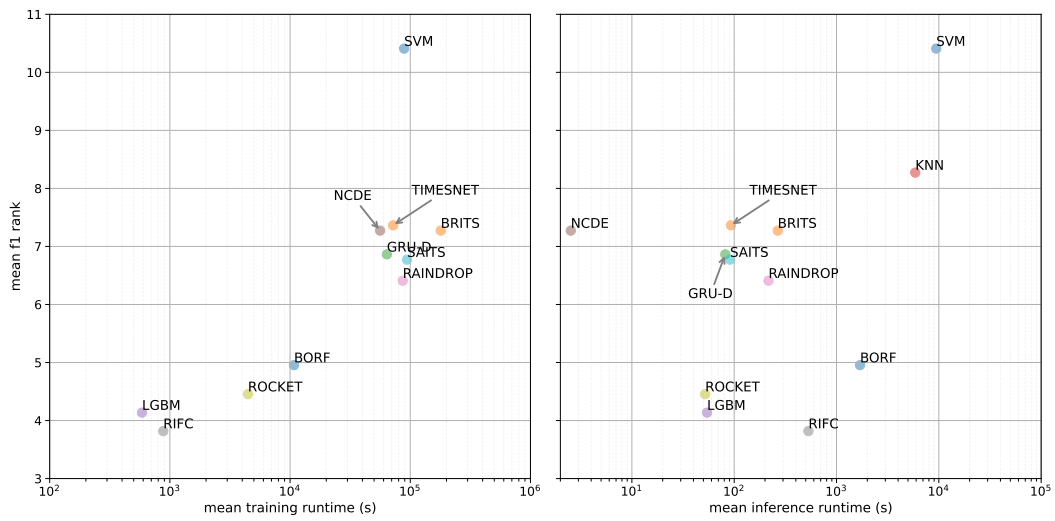
(a) Unequal Length.



(b) Shift.

Figure 18: Average F1 rank (lower is better) vs. training and inference runtimes (lower is better) for subsets of datasets. Best values are on the bottom-left of each plot.





(a) Ragged Sampling.

Figure 19: Average F1 rank (lower is better) vs. training and inference runtimes (lower is better) for subsets of datasets. Best values are on the bottom-left of each plot.

## D Array Structures

We report a summary of the main formats used to represent regular and irregular time series data in the literature in Table 8.

Table 8: Overview of the main formats used to represent regular and irregular time series data in the literature, categorized by tensor type. The table details the underlying data structures (classes), the software libraries that implement them, their usage across the time series libraries considered in this study, and their support for timestamps and tensor operations.

Type	Format	Library	Class	Usage	Timestamps	Tensor Ops.
Dense	3D Tensor	numpy	Array	aeon	✗	✓
		numpy	Array	sktime	✗	✓
		numpy	Array	tslearn	✗	✓
		numpy	MaskedArray	-	✗	✓
		jax	Array	diffraction	✓*	✓
		tensorflow	Array	-	✗	✓
		torch	Tensor	pypots	✗	✓
Ragged	3D Tensor	awkward	AwkwardArray	-	✗	✓
		tensorflow	RaggedTensor	-	✗	✓
		torch	NestedTensor	-	✗	✓
		zarr	RaggedArray	-	✗	✓
		pyarrow	ListArray	-	✗	✓
Sparse	3D Tensor	sparse	GCXS	-	✗	✓
		sparse	DOK	-	✗	✓
		sparse	COO	-	✗	✓
Other	Nested List	python	List[Array]	aeon	✗	✗
	3D tensor**	xarray	Dataset	-	✓	✓
	Long	pandas	DataFrame	sktime	✓	✗
	MultiIndex	pandas	DataFrame	sktime	✓	✗

\* only as a separate channel

\*\* with additional tensors for static variables

## E Quick Guide

In the following, we report a quick start guide and some simple workflow notebooks. More examples and tutorials are available at <https://fspinna.github.io/pyrregular/>.

You can install via pip with:

```
pip install pyrregular
```

For third-party models use:

```
pip install pyrregular[models]
```

### List datasets

If you want to see all the datasets available, you can use the `list_datasets` function:

```
from pyrregular import list_datasets  
  
df = list_datasets()
```

### Load a dataset

To load a dataset, you can use the `load_dataset` function. For example, to load the "Garment" dataset, you can do:

```
from pyrregular import load_dataset  
  
df = load_dataset("Garment.h5")
```

### Classification

To use the dataset for classification, you can just "densify" it:

```
from pyrregular import load_dataset  
  
df = load_dataset("Garment.h5")  
X, _ = df.irr.to_dense()  
y, split = df.irr.get_task_target_and_split()  
  
X_train, X_test = X[split != "test"], X[split == "test"]  
y_train, y_test = y[split != "test"], y[split == "test"]  
  
# We have ready-to-go models from various libraries:  
from pyrregular.models.rocket import rocket_pipeline  
  
model = rocket_pipeline  
model.fit(X_train, y_train)  
model.score(X_test, y_test)
```

## Notebook: Basic Workflow

```
[1]: import xarray as xr
```

### List available datasets

To view available datasets, you can use the `list_datasets` function.

```
[2]: from pyrregular import list_datasets
```

```
[3]: print(list_datasets())
```

```
['Abf.h5', 'AllGestureWiimoteX.h5', 'AllGestureWiimoteY.h5',  
'AllGestureWiimoteZ.h5', 'Animals.h5', 'AsphaltObstaclesCoordinates.h5',  
'AsphaltPavementTypeCoordinates.h5', 'AsphaltRegularityCoordinates.h5',  
'CharacterTrajectories.h5', 'DodgerLoopDay.h5',  
'DodgerLoopGame.h5', 'DodgerLoopWeekend.h5', 'Garment.h5',  
'GeolifeSupervised.h5', 'GestureMidAirD1.h5', 'GestureMidAirD2.h5',  
'GestureMidAirD3.h5', 'GesturePebbleZ1.h5', 'GesturePebbleZ2.h5',  
'JapaneseVowels.h5', 'Ldfpa.h5', 'MelbournePedestrian.h5', 'Mimic3.h5',  
'PLAID.h5', 'Pamap2.h5', 'Physionet2012.h5', 'Physionet2019.h5',  
'PickupGestureWiimoteZ.h5', 'Seabirds.h5', 'ShakeGestureWiimoteZ.h5',  
'SpokenArabicDigits.h5', 'Taxi.h5', 'Vehicles.h5']
```

### Loading the dataset from the online repository

Loading a dataset is as from the online repo (<https://huggingface.co/datasets/splandi/pyrregular>) is as simple as calling the `load_dataset` function with the dataset name.

```
[4]: from pyrregular import load_dataset
```

```
[64]: ds = load_dataset("Garment.h5")
```

The dataset is loaded as an xarray dataset. The dataset is saved in the default os cache directory, which can be found with:

```
import pooch  
print(pooch.os_cache("pyrregular"))
```

You can also use xarray to directly load a local file. In this case, you have to specify our backend as `pyrregular` in the `engine` argument.

```
import xarray as xr  
ds = xr.load_dataset("path/to/file.h5", engine="pyrregular")
```

You can view the underlying DataArray by calling the `data` variable.

```
[65]: da = ds.data
```

```
[66]: da
```

```
[66]: <xarray.DataArray 'data' (ts_id: 24, signal_id: 9, time_id: 59)> Size: 329kB
      <C00: shape=(24, 9, 59), dtype=float64, nnz=10267, fill_value=nan>
Coordinates:
      day                (time_id) <U9 2kB 'Thursday' ... 'Wednesday'
      department         (ts_id) <U9 864B 'finishing' ... 'sweing'
      productivity_binary (ts_id) int32 96B 1 0 1 1 1 1 1 1 ... 1 1 0 0 0 0 1
      productivity_class  (ts_id) <U4 384B 'high' 'low' ... 'low' 'high'
      productivity_numerical (ts_id) float32 96B 0.8126 0.6283 ... 0.7005 0.7503
      quarter            (time_id) <U8 2kB 'Quarter1' ... 'Quarter2'
      * signal_id         (signal_id) <U21 756B 'idle_men' ... 'wip'
      split              (ts_id) <U5 480B 'train' 'train' ... 'train' 'train'
      team               (ts_id) int32 96B 1 10 11 12 2 3 4 ... 3 4 5 6 7 8 9
      * time_id           (time_id) datetime64[ns] 472B 2015-01-01T01:00:00...
      * ts_id             (ts_id) <U12 1kB 'finishing_1' ... 'sweing_9'
Attributes:
      _fixed_at: 2024-12-04T21:50:44.408790-12:00
      _is_fixed: True
      author: [Abdullah Al Imran, Md Shamsur Rahim, Tanvir Ahmed]
      configs: {'default': {'task': 'classification', 'split': 'split', 'tar...
      license: CC BY 4.0
      source: https://archive.ics.uci.edu/dataset/597/productivity+predicti...
      title: Productivity Prediction of Garment Employees
```

```
[67]: # the shape is (n_time_series, n_channels, n_timestamps)
      da.shape
```

```
[67]: (24, 9, 59)
```

```
[68]: # the array is stored as a sparse array
      da.data
```

```
[68]: <C00: shape=(24, 9, 59), dtype=float64, nnz=10267, fill_value=nan>
```

```
[69]: # dimensions contain the time series ids, signal ids and timestamps
      da.dims
```

```
[69]: ('ts_id', 'signal_id', 'time_id')
```

```
[70]: # e.g., these are the time series ids
      da["ts_id"].data
```

```
[70]: array(['finishing_1', 'finishing_10', 'finishing_11', 'finishing_12',
          'finishing_2', 'finishing_3', 'finishing_4', 'finishing_5',
          'finishing_6', 'finishing_7', 'finishing_8', 'finishing_9',
          'sweing_1', 'sweing_10', 'sweing_11', 'sweing_12', 'sweing_2',
          'sweing_3', 'sweing_4', 'sweing_5', 'sweing_6', 'sweing_7',
          'sweing_8', 'sweing_9'], dtype='<U12')
```

```
[72]: # there are also static variables, such as the class
da["productivity_binary"].data
```

```
[72]: array([1, 0, 1, 1, 1, 1, 1, 1, 0, 0, 0, 0, 1, 1, 1, 1, 1, 1, 0, 0, 0,
        0, 1], dtype=int32)
```

```
[74]: # the train/test split
da["split"].data
```

```
[74]: array(['train', 'train', 'test', 'train', 'train', 'test', 'train',
            'train', 'train', 'test', 'train', 'train', 'test', 'train',
            'train', 'test', 'train', 'train', 'train', 'train', 'test',
            'train', 'train', 'train'], dtype='<U5')
```

```
[75]: # all the coordinates can be accessed via the `coords` variable
da.coords
```

```
[75]: Coordinates:
      day                (time_id) <U9 2kB 'Thursday' ... 'Wednesday'
      department        (ts_id) <U9 864B 'finishing' ... 'sweing'
      productivity_binary (ts_id) int32 96B 1 0 1 1 1 1 1 1 ... 1 1 0 0 0 0 1
      productivity_class  (ts_id) <U4 384B 'high' 'low' ... 'low' 'high'
      productivity_numerical (ts_id) float32 96B 0.8126 0.6283 ... 0.7005 0.7503
      quarter            (time_id) <U8 2kB 'Quarter1' ... 'Quarter2'
      * signal_id         (signal_id) <U21 756B 'idle_men' ... 'wip'
      split              (ts_id) <U5 480B 'train' 'train' ... 'train' 'train'
      team               (ts_id) int32 96B 1 10 11 12 2 3 4 ... 3 4 5 6 7 8 9
      * time_id           (time_id) datetime64[ns] 472B 2015-01-01T01:00:00...
      * ts_id             (ts_id) <U12 1kB 'finishing_1' ... 'sweing_9'
```

```
[76]: # metadata contains informations about the datasets and tasks
da.attrs
```

```
[76]: {'_fixed_at': '2024-12-04T21:50:44.408790-12:00',
      '_is_fixed': True,
      'author': [Abdullah Al Imran, Md Shamsur Rahim, Tanvir Ahmed],
      'configs': {'default': {'task': 'classification',
                              'split': 'split',
                              'target': 'productivity_binary'},
                  'regression': {'task': 'regression',
                                  'split': 'split',
                                  'target': 'productivity_numerical'}}},
      'license': 'CC BY 4.0',
      'source': 'https://archive.ics.uci.edu/dataset/597/productivity+prediction+of+g
arment+employees',
      'title': 'Productivity Prediction of Garment Employees'}
```

## Data Handling and Plotting

Data can be accessed with standard xarray methods.

```
[77]: import matplotlib.pyplot as plt
import numpy as np
```

```
[78]: # the first time series
da[0]
```

```
[78]: <xarray.DataArray 'data' (signal_id: 9, time_id: 59)> Size: 9kB
<C00: shape=(9, 59), dtype=float64, nnz=392, fill_value=nan>
Coordinates:
  day                (time_id) <U9 2kB 'Thursday' ... 'Wednesday'
  department         <U9 36B 'finishing'
  productivity_binary int32 4B 1
  productivity_class  <U4 16B 'high'
  productivity_numerical float32 4B 0.8126
  quarter            (time_id) <U8 2kB 'Quarter1' ... 'Quarter2'
  * signal_id        (signal_id) <U21 756B 'idle_men' ... 'wip'
  split              <U5 20B 'train'
  team               int32 4B 1
  * time_id          (time_id) datetime64[ns] 472B 2015-01-01T01:00:00...
  ts_id              <U12 48B 'finishing_1'
Attributes:
  _fixed_at: 2024-12-04T21:50:44.408790-12:00
  _is_fixed: True
  author: [Abdullah Al Imran, Md Shamsur Rahim, Tanvir Ahmed]
  configs: {'default': {'task': 'classification', 'split': 'split', 'tar...
  license: CC BY 4.0
  source: https://archive.ics.uci.edu/dataset/597/productivity+predicti...
  title: Productivity Prediction of Garment Employees
```

```
[79]: # the first channel of the first time series
da[0, 0]
```

```
[79]: <xarray.DataArray 'data' (time_id: 59)> Size: 784B
<C00: shape=(59,), dtype=float64, nnz=49, fill_value=nan>
Coordinates:
  day                (time_id) <U9 2kB 'Thursday' ... 'Wednesday'
  department         <U9 36B 'finishing'
  productivity_binary int32 4B 1
  productivity_class  <U4 16B 'high'
  productivity_numerical float32 4B 0.8126
  quarter            (time_id) <U8 2kB 'Quarter1' ... 'Quarter2'
  signal_id          <U21 84B 'idle_men'
  split              <U5 20B 'train'
  team               int32 4B 1
```

```

* time_id          (time_id) datetime64[ns] 472B 2015-01-01T01:00:00...
  ts_id            <U12 48B 'finishing_1'
Attributes:
  _fixed_at: 2024-12-04T21:50:44.408790-12:00
  _is_fixed: True
  author: [Abdullah Al Imran, Md Shamsur Rahim, Tanvir Ahmed]
  configs: {'default': {'task': 'classification', 'split': 'split', 'tar...
  license: CC BY 4.0
  source: https://archive.ics.uci.edu/dataset/597/productivity+predicti...
  title: Productivity Prediction of Garment Employees

```

```
[80]: # to access the underlying sparse vector
      da[0, 0].data
```

```
[80]: <C00: shape=(59,), dtype=float64, nnz=49, fill_value=nan>
```

```
[87]: # to access the underlying dense vector
      da[0, 4].data.todense()
```

```
[87]: array([ 8.,  8.,  8.,  8.,  8.,  8.,  8.,  8.,  8.,  8.,  2.,  8.,  8.,
            8., nan, nan, nan,  8., 25.,  8.,  8., 10., 10., 10., 10., 15.,
            19., 19., 10., 10., 12., 10., 10., 10., 12., 12., 12., 12.,  8.,
            nan, nan, nan, nan, 12., nan, nan, nan,  8.,  8.,  8.,  8.,  8.,
            8.,  8.,  8.,  8.,  8.,  8.,  8.])
```

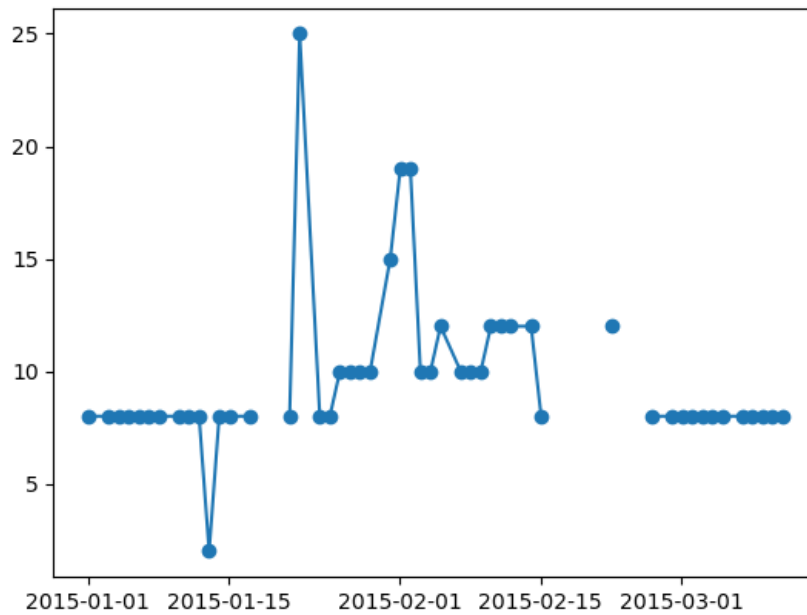
```
[89]: # this vector contains a lot of nans, which are the padding necessary to have
      ↳ shared timestamps w.r.t. the whole dataset
      np.isnan(da[0, 4].data.todense()).sum()
```

```
[89]: 10
```

```
[90]: plt.plot(da[0, 4]["time_id"], da[0, 4], marker="o")
```

```
[90]: [<matplotlib.lines.Line2D at 0x14eb06990>]
```



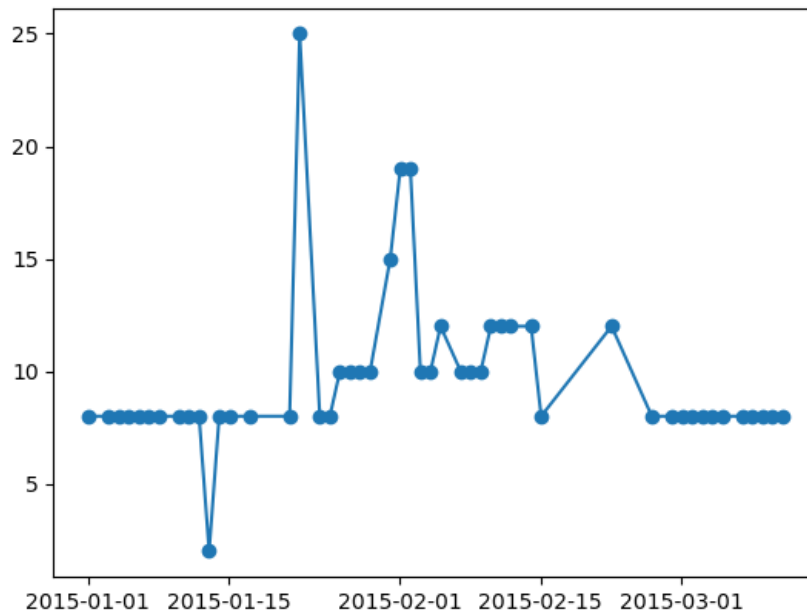


```
[92]: # using the custom ".irr" accessor, we can filter out the nans to the minimum
      ↪ amount possible due to raggedness
      np.isnan(da.irr[0, 4].data.todense()).sum()
```

[92]: 0

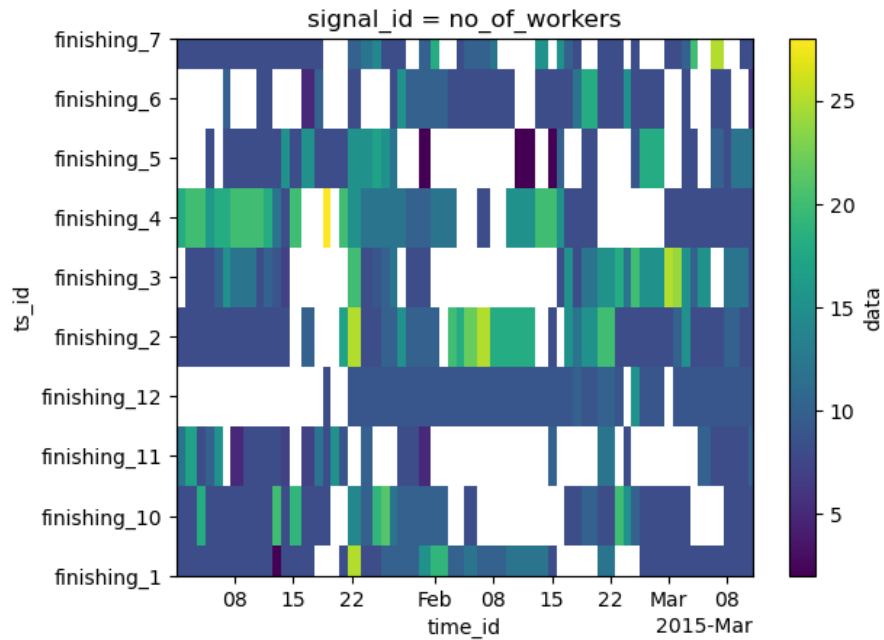
```
[93]: plt.plot(da.irr[0, 4]["time_id"], da.irr[0, 4], marker="o")
```

[93]: [<matplotlib.lines.Line2D at 0x14eb6b230>]



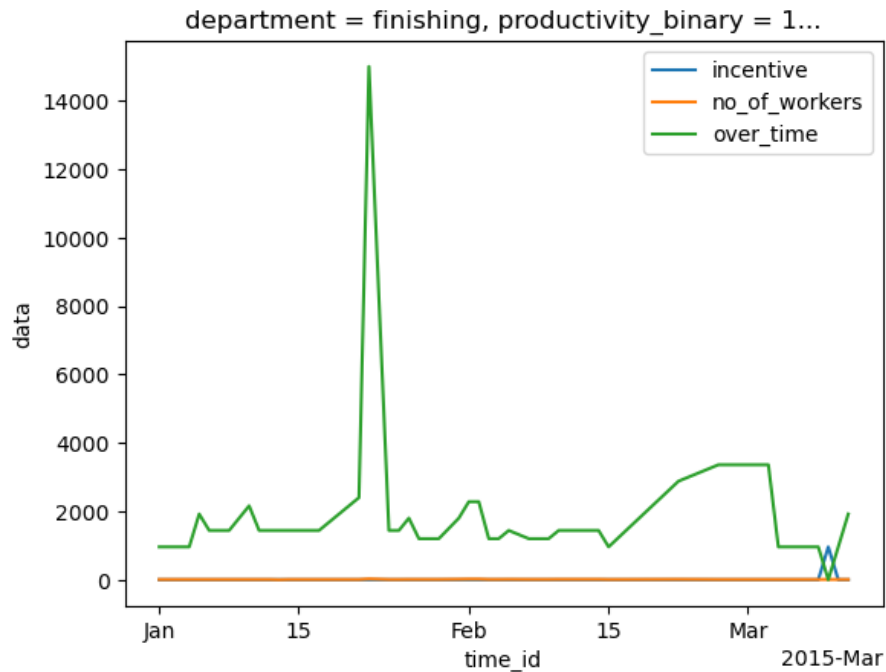
```
[94]: # the fourth channel first 10 time series of the dataset, as a heatmap
da.irr[:10, 4].plot()
```

```
[94]: <matplotlib.collections.QuadMesh at 0x14dcf3680>
```



```
[103]: # plotting some channels
da.irr[0, 2].plot(label=da.coords["signal_id"][2].item())
da.irr[0, 4].plot(label=da.coords["signal_id"][4].item())
da.irr[0, 5].plot(label=da.coords["signal_id"][5].item())
plt.legend()
```

```
[103]: <matplotlib.legend.Legend at 0x16ea32870>
```



## Downstream Tasks

The xarray is nice, but not supported by basically any downstream library. Thus, we can convert it into a numpy array.

```
[104]: %%time
# time series data, timestamps
X, T = da.irr.to_dense(
    normalize_time=True, # normalize the time index to [0, 1]
)
```

CPU times: user 2.23 s, sys: 79 ms, total: 2.31 s  
Wall time: 2.34 s

```
[106]: # the shape is (n_time_series, n_channels, n_timestamps), timestamps are
↳ returned as a separate channel, for downstream methods that are able to use
↳ them
X.shape, T.shape
```

```
[106]: ((24, 9, 59), (24, 1, 59))
```

```
[107]: # static variables
Z = da.coords.to_dataset()[["split", "productivity_binary"]].to_pandas()
Z.head()
```

```
[107]:
```

	split	productivity_binary	department	productivity_class	\
ts_id					
finishing_1	train	1	finishing	high	
finishing_10	train	0	finishing	low	
finishing_11	test	1	finishing	high	
finishing_12	train	1	finishing	high	
finishing_2	train	1	finishing	high	

	productivity_numerical	team
ts_id		
finishing_1	0.812625	1
finishing_10	0.628333	10
finishing_11	0.874028	11
finishing_12	0.922840	12
finishing_2	0.819271	2

```
[108]: # target and split
y, split = da.irr.get_task_target_and_split()
```

### Train-test split

```
[111]: X_train, X_test = X[split != "test"], X[split == "test"]
y_train, y_test = y[split != "test"], y[split == "test"]
X_train.shape, y_train.shape, X_test.shape, y_test.shape
```

```
[111]: ((18, 9, 59), (18,), (6, 9, 59), (6,))
```

### Classification

We have several ready-to-use classifiers in the `pyrregular` package. Be sure to install the required dependencies.

```
[118]: from pyrregular.models.rocket import rocket_pipeline
```

```
[119]: %%time
model = rocket_pipeline
model.fit(X_train, y_train)
model.score(X_test, y_test)
```

```
[119]: 0.6666666666666666
```

## Notebook: Dataset Conversion

### The “Long Format”

The basic format to convert any dataset to our representation is the long format. The long format is simply a tuple:

```
(time_series_id, channel_id, timestamp, value, static_var_1, static_var_2, ...).
```

If your dataset contains rows that are in this format, you are almost good to go. Else, there will be a little bit of preprocessing to do.

#### Case 1. (easy) Your dataset is already in the long format

Let’s assume for now your dataset is already in this form. Here is a minimal working example.

```
[28]: import pandas as pd
import numpy as np
```

```
[29]: df = pd.DataFrame(
    {
        "time_series_id": np.random.choice(["A", "B", "C"], size=100),
        "channel_id": np.random.choice(["X", "Y", "Z"], size=100),
        "timestamp": pd.date_range("2023-01-01", periods=100, freq="H"),
        "value": np.random.randn(100),
    }
)
df["labels"] = df["time_series_id"].map(
    {"A": 0, "B": 1, "C": 1}
) # let's say we have labels
df.head()
```

```
/var/folders/kj/v66zvn217x31k61x631t02q40000gn/T/ipykernel_11325/3078918095.py:5
: FutureWarning: 'H' is deprecated and will be removed in a future version,
please use 'h' instead.
"timestamp": pd.date_range("2023-01-01", periods=100, freq="H"),
```

```
[29]:  time_series_id channel_id      timestamp      value  labels
0             B          Y 2023-01-01 00:00:00  0.105162      1
1             B          Z 2023-01-01 01:00:00 -0.573337      1
2             B          X 2023-01-01 02:00:00 -1.973967      1
3             C          Y 2023-01-01 03:00:00  0.656065      1
4             A          Y 2023-01-01 04:00:00 -0.500246      0
```

```
[30]: # Let's save this dataframe to a CSV file
df.to_csv("your_original_dataset.csv", index=False)
```

```
[31]: # the csv file can be converted to our format using our interface

from pyrregular.io_utils import read_csv
```

```

from pyrregular.reader_interface import ReaderInterface
from pyrregular.accessor import IrregularAccessor

class YourDataset(ReaderInterface):
    @staticmethod
    def read_original_version(verbose=False):
        return read_csv(
            filenames="your_original_dataset.csv",
            ts_id="time_series_id",
            time_id="timestamp",
            signal_id="channel_id",
            value_id="value",
            dims={
                "ts_id": [
                    "labels"
                ], # static variable that depends on the time series id
                "signal_id": [],
                "time_id": [],
            },
            time_index_as_datetime=False,
            verbose=verbose,
        )

```

```

[32]: da = YourDataset.read_original_version(True)
      da

```

Getting dataset metadata: 0it [00:00, ?it/s]

Reading dataset: 0% | 0/100 [00:00<?, ?it/s]

```

[32]: <xarray.DataArray (ts_id: 3, signal_id: 3, time_id: 100)> Size: 3kB
      <C00: shape=(3, 3, 100), dtype=float64, nnz=100, fill_value=nan>
      Coordinates:
        * time_id    (time_id) <U19 8kB '2023-01-01 00:00:00' ... '2023-01-05 03:00...'
          labels     (ts_id) int64 24B 0 1 1
        * ts_id      (ts_id) <U1 12B 'A' 'B' 'C'
        * signal_id  (signal_id) <U1 12B 'X' 'Y' 'Z'

```

If you don't know if a variable is static, or to which dimension it depends from, you can check it.

```

[33]: from pyrregular.data_utils import infer_static_columns

      infer_static_columns(df, "time_series_id")

```

```

[33]: ['labels']

```

The dataset can be saved with our custom accessor

```
[34]: da.irr.to_hdf5("your_dataset.h5")
```

And then loaded directly with xarray

```
[35]: import xarray as xr
```

```
[36]: da2 = xr.load_dataset("your_dataset.h5", engine="pyrregular")
da2
```

```
/Users/francesco/github/irregular_ts/irregular_ts/accessor.py:9:
AccessorRegistrationWarning: registration of accessor <class
'irregular_ts.accessor.IrregularAccessor'> under name 'irr' for type <class
'xarray.core.dataarray.DataArray'> is overriding a preexisting attribute with
the same name.
  @xr.register_dataarray_accessor("irr")
```

```
[36]: <xarray.Dataset> Size: 11kB
Dimensions:    (ts_id: 3, signal_id: 3, time_id: 100)
Coordinates:
  labels      (ts_id) int32 12B 0 1 1
  * signal_id (signal_id) <U1 12B 'X' 'Y' 'Z'
  * time_id   (time_id) <U19 8kB '2023-01-01 00:00:00' ... '2023-01-05 03:00...'
  * ts_id     (ts_id) <U1 12B 'A' 'B' 'C'
Data variables:
  data        (ts_id, signal_id, time_id) float64 3kB <C00: nnz=100,
fill_value=nan>
```

## Case 2. Your dataset is not in the long format

Let's say you have a 3d numpy array, containing the time series, and a numpy array containing only the labels.

```
[37]: import numpy as np

shape = (10, 2, 100) # 10 time series, 2 channels, 100 timestamps
data = np.full(shape, np.nan)
mask = np.random.rand(*shape) < 0.35
data[mask] = np.random.randn(mask.sum())
labels = np.random.randint(0, 2, shape[0])

np.save("your_more_complex_dataset.npy", data)
np.save("your_more_complex_dataset_labels.npy", labels)

data.shape, labels.shape
```

```
[37]: ((10, 2, 100), (10,))
```

You need only a function that takes the data and the labels, and returns a dataframe in the long format, yielding it row by row.



```
[38]: def read_your_dataset(filenamees):
    data = np.load(filenamees["data"])
    labels = np.load(filenamees["labels"])
    ts_ids, signal_ids, timestamps = np.indices(shape)
    ts_ids, signal_ids, timestamps = ts_ids.ravel(), signal_ids.ravel(),
    ↪ timestamps.ravel()

    for ts_id, signal_id, timestamp in zip(ts_ids, signal_ids, timestamps):
        value = data[ts_id, signal_id, timestamp]
        if np.isnan(value):
            continue
        label = labels[ts_id]
        yield dict(
            time_series_id=ts_id,
            channel_id=signal_id,
            timestamp=timestamp,
            value=value,
            labels=label,
        )
```

```
[39]: from pyrregular.io_utils import read_csv
    from pyrregular.reader_interface import ReaderInterface
    from pyrregular.accessor import IrregularAccessor

    class YourDataset(ReaderInterface):
        @staticmethod
        def read_original_version(verbose=False):
            return read_csv(
                filenames={
                    "data": "your_more_complex_dataset.npy",
                    "labels": "your_more_complex_dataset_labels.npy",
                },
                ts_id="time_series_id",
                time_id="timestamp",
                signal_id="channel_id",
                value_id="value",
                dims={
                    "ts_id": [
                        "labels"
                    ], # static variable that depends on the time series id
                    "signal_id": [],
                    "time_id": [],
                },
                reader_fun=read_your_dataset,
                time_index_as_datetime=False,
                verbose=verbose,
                attrs={
```

```

        "authors": "Bond, James Bond", # you can add any attribute you want
    }
)

```

```

[40]: da = YourDataset.read_original_version(True)
      da

```

Getting dataset metadata: 0it [00:00, ?it/s]

Reading dataset: 0%| | 0/720 [00:00<?, ?it/s]

```

[40]: <xarray.DataArray (ts_id: 10, signal_id: 2, time_id: 100)> Size: 23kB
      <C00: shape=(10, 2, 100), dtype=float64, nnz=720, fill_value=nan>
      Coordinates:
        * time_id      (time_id) int64 800B 0 1 2 3 4 5 6 7 ... 92 93 94 95 96 97 98 99
          labels        (ts_id) int64 80B 0 0 0 1 1 1 0 1 1 0
        * ts_id         (ts_id) <U21 840B '0' '1' '2' '3' '4' '5' '6' '7' '8' '9'
        * signal_id     (signal_id) <U21 168B '0' '1'
      Attributes:
        authors:      Bond, James Bond

```